MT1 and MT2 melatonin receptors are expressed in nonoverlapping neuronal populations.

Paul Klosen, Sarawut Lapmanee, Carole Schuster, Béatrice Guardiola, David Hicks, Paul Pevet, Marie Paule Felder-schmittbuhl

Journal of Pineal Research
Molecular, Biological, Physiological and Clinical Aspects of Melatonin

MT1 and MT2 melatonin receptors are expressed in non-overlapping neuronal populations

Journal:	*Journal of Pineal Research*
Manuscript ID	JPI-OM-02-19-0046.R1
Manuscript Type:	Original Manuscript
Date Submitted by the Author:	n/a
Complete List of Authors:	Klosen, Paul; University of Strasbourg, Institute of Cellular and Integrative Neurosciences Sawarut, lapmanee; University of Strasbourg, CNRS, INCI Schuster-Klein, Carole; ADIR - Servier Research group Guardiola-Lemaitre, Beatrice; ADIR - Servier research group Hicks, David; University of Strasbourg, CNRS Pévet, Paul; Institut des Neurosciences Cellulaires et Intégratives, UPR 3212 CNRS Felder-Schmittbuhl, Marie Paule; University of Strasbourg, CNRS, INCI
Keywords:	Melatonin,, Melatonin receptor subtypes (MT1, MT2), transgenic mice, immunohistochemistry, tissue distribution

Title: **MT1 and MT2 melatonin receptors are expressed in non-overlapping neuronal populations**

Short title**: Identification of MT1 or MT2 receptor expressing cells.**

Authors:
P.Klosen* 1, S Lapmanee 1#, C. Schuster 2, B. Guardiola 2, D. Hicks 1, P. Pevet*,**1 M.P. Felder-Schmittbuhl*1
1) Institute for Cellular and Integrative Neurosciences (UPR 3212), CNRS and University of Strasbourg, Strasbourg France
2) ADIR - SERVIER Research Group, Suresnes, France.
#Present address: Faculty of Medicine, Siam University, Bangkok, Thailand
* these authors contributed equally to this work.

Contact information** Correspondence: Paul Pevet, Institute for Cellular and Integrative Neurosciences (UPR 3212), CNRS and University of Strasbourg, Strasbourg France; Tel (33)632982571; pevet@inci-cnrs.unistra.fr

Abstract

Melatonin (MLT) exerts its physiological effects principally through two high-affinity membrane receptors MT1 and MT2. Understanding the exact mechanism of MLT action necessitates the use of highly selective agonists/antagonists to stimulate/inhibit a given MLT receptor. The respective distribution of MT1 and MT2 within the CNS and elsewhere is controversial, and here we used a "knock-in" strategy replacing MT1 or MT2 coding sequences with a LacZ reporter. The data show striking differences in the distribution of MT1 and MT2 receptors in the mouse brain: whereas the MT1 subtype was expressed in very few structures (notably including the suprachiasmatic nucleus and *pars tuberalis*), MT2 subtype receptors were identified within numerous brain regions including the olfactory bulb, forebrain, hippocampus, amygdala and superior colliculus. Co-expression of the two subtypes was observed in very few structures, and even within these areas they were rarely present in the same individual cell. In conclusion, the expression and distribution of MT2 receptors are much more widespread than previously thought, and there is virtually no correspondence between MT1 and MT2 cellular expression. The precise phenotyping of cells/neurons containing MT1 or MT2 receptor subtypes opens new perspectives for the characterization of links between MLT brain targets, MLT actions and specific MLT receptor subtypes.

Keywords

Melatonin, Melatonin receptor subtypes (MT1, MT2), transgenic mice, immunohistochemistry, tissue distribution

Introduction

Experiments in animals as well as clinical or epidemiological studies in humans demonstrate that disorders of rhythmicity can cause a variety of pathologies, and are known to impair processes involved in metabolism and can lead to cardiovascular disease and cancer (1-5). It is now known that a complex multi-oscillatory circadian network, orchestrated by a master clock located in the suprachiasmatic nuclei (SCN) of the hypothalamus, governs optimal and anticipatory temporal organization of functions in mammals (6,7). Nervous and endocrine effectors receive signals from the master clock via nervous and endocrine pathways and translate them into hormonal, physiological or behavioral responses in specialized structures (8, 9). Among these structures is the pineal gland, which secretes the hormone melatonin (MLT)*. Being tightly controlled by the SCN through a well-characterized multi-synaptic neural pathway, MLT is synthesized by the pineal gland during the night (14, 15). MLT is immediately released into the general circulation after its synthesis, hence circulating MLT is an endocrine signal from the SCN providing a nocturnal/ circadian message to the organism. Although MLT is not the only endocrine output of the circadian clock it constitutes the most stable one, directly measurable in saliva and plasma, and thus provides a robust and reliable indicator of SCN clock function. Furthermore, the duration of the nocturnal peak of MLT secretion also reflects the length of the night, and changes in MLT duration are integrated by the brain to measure photoperiodic time (16-21). The daily profile of MLT secretion conveys internal information used for both circadian and seasonal temporal organization. Although MLT (N-Acetyl-5-Methoxytryptamine) has been credited with many properties since its identification (22), it is the finding that MLT acts as both SCN clock output and internal synchronizer within the circadian clock network (9) which strongly suggests that its major function is to act as a 'time-giver". MLT acts through several mechanisms and understanding its physiological function depends on how and where its actions are exerted. In view of its amphiphilic nature, MLT is able to enter any tissue and cellular compartment. At higher concentrations (μM and above), the pharmacological actions of MLT are thought to be mediated via interactions with intracellular proteins such as calmodulin or quinone reductase (QR2) (23, 24). Also, at very high concentrations MLT appears to be a potent free radical scavenger (25). These antioxidant properties, of which the physiological significance still remains to be established, are independent from the 'time-giving' action of the hormone.

As for other hormones, MLT exerts its physiological effects principally through high-affinity receptors. Since 1987, with the use of 2-[^{125}I] MLT as a highly specific ligand, binding sites have been reported in a large number of structures within the brain and periphery, with a great variability in number, localization and density among species (26-30). Different subtypes of mammalian MLT receptors have been cloned (31, 32) and characterized pharmacologically (32, 33). The MT1 and the MT2 subtypes are members of the seven-transmembrane G-protein-coupled receptor family and exhibit sub-nanomolar affinity for MLT (32-34). The MT3 subtype does not correspond to a membrane receptor but to a low affinity binding site on QR2 (24). The two different cloned MLT membrane receptor subtypes possess intrinsic differences, evidenced by different signal transduction pathways as well as their differential tissue distribution. The widespread experimental use of

---

***Foot-note :** Numerous other MLT sources have been identified beside the pineal gland (retina, Harderian gland, gastrointestinal tract, red blood cells, platelets, mononuclear cells, etc. (10-13)). The pineal gland, however, is the main source of the nocturnal peak of circulating MLT, as evidenced by the lack of detectable levels in the blood after pinealectomy. Whether MLT in these other organs has autocrine or paracrine effects is also an important question. For that, identification of MLT receptors at the cellular level would also be of interest.*

2-[^{125}I]-iodo-melato-nin receptor binding in rodents, monkey and human, as well as the great number of structurally different MLT receptor ligands developed, have already provided great

progress in understanding the action and function of MLT. However, understanding the links between specific target sites for MLT, receptor subtypes, and particular physiological actions is still challenging. The continuing search for alternative radioligands (35) and the development of MT1- or MT2-selective ligands (36-38) will be of great help in the future. Knockout animals (39) have also allowed the functional characterization of MT1 and MT2 receptors that, even if far from being complete, has highlighted some differential roles for the two subtypes.

In situ hybridization and reverse transcription polymerase chain reaction (RT-PCR) analysis have also been used to analyze the distribution of mRNA coding for the two receptor subtypes. Most expression sites have only been described at the macroscopical level (40-45). With the exception of the *pars tuberalis* (46), and the SCN in Siberian Hamster (47), none of these techniques achieve sufficient cellular resolution to identify the individual cells/neurons concerned. Immunohistochemical approaches have generated detailed mapping at the cellular level of both MLT receptors in the rat (48, 49). However the questionable specificity of most MLT receptor antibodies has seriously hampered obtaining convincing data. Knowledge of the cell types that contain MT1 and/or MT2 receptors is critical in defining their potential differential roles and to revive long-standing interests regarding possible therapeutic applications for MLT. Transgenic mice expressing marker enzymes under control of the endogenous MT1 or MT2 gene promoters should allow precise phenotyping of the cells containing MLT receptors. Previous attempts using bacterial artificial chromosome transgenesis did not provide convincing data (50). We have thus used a specific reporter "knock-in" strategy replacing the MT1 or MT2 coding sequence with the LacZ reporter enzyme in the endogenous loci without modifying the endogenous upstream and downstream regulatory elements

Materials and Methods

Generation of Mtnr1a and Mtnr1b reporter mice

Targeted ES cells generated in the KnockOut Mouse Project (KOMP), were derived from the C57BL/6NTac mouse strain following the deletion strategy already described by (51). In the recombinant alleles (Mtnr1a$^{tm1(KOMP)Vlcg}$ and Mtnr1b$^{tm1(KOMP)Vlcg}$) of both *Mtnr1a* and *Mtnr1b*, a cassette (ZEN_Ubl) containing a modified *E. coli* β-galactosidase open reading frame in tandem with a selection gene (Neomycine resistance) replaces the coding sequence of the melatonin receptor (including intron 1-2). This cassette is inserted precisely at the original endogenous start codon and ends after the original stop codon (respectively 45 and 40 bp downstream of the stop) (Fig.1). Mice carrying the recombinant allele were generated by classical ES cell-based/germline transmission procedure at the Institut Clinique de la Souris, Illkirch, France for *Mtnr1a* and at the KOMP Repository (UC Davis, US) for *Mtrn1b* (MGI ID: 4399541). In both cases, the selection gene was eliminated by breeding with mice expressing the CRE recombinase. The 5' and 3' junctions between the *Mtnr1a*/*Mtnr1b* genes and the inserted reporter cassettes were confirmed by PCR amplification and sequencing.

Animals and Housing

Mice carrying the recombinant alleles were backcrossed on a C57BL/6J background and segregation of the *rd8* mutation (initially present in the C57BL/6NTac ES cells) was verified by genotyping (52). All mice processed for histological analysis were from the 5th generation backcross and beyond. Mice homozygous for the knockin allele were generated on an *ad hoc* basis by heterozygote breeding. Likewise, heterozygote mice on a F1 C57BL/6J x C3H/HeN or a F1 C57BL/6J x CBA/J background were generated by crossing B6

heterozygotes to C3H melatonin proficient, *rd1/rd1* mice. All backcross mice were purchased from Charles River, France.

Mouse Genotyping

For both lines, genotyping was performed on DNA isolated from tail biopsies by the Hot Shot technique, by using primers and PCR conditions optimized by the suppliers (ICS for *Mtnr1a*, KOMP for *Mtnr1b*). For both genes, DNA samples were amplified separately for the wild type (*wt*) and the knock-in (*ki*) allele. For *Mtnr1a* primer sequences were: Xf 5'-CAAGTTGCTGGGCAGTGGACAGCAG and Wr 5'-CTTCTTGTTGCGGTACACAGACAGG for *wt* (425 bp amplicon) and Xf2 5'-GCGGGAGGGCCATAAAAAGTGGC and Sr 5'-CTAGTCTGTTCAGCTGTGTCACACC for *ki* (196 bp amplicon). Both PCR reactions were performed for 35 cycles of 30 s at 95°C, 30 s at 59 °C, 1 min at 72°C using Taq polymerase (Euromedex). For *Mtnr1b* primer sequences were: Mtnr1b-wtF 5'-AAGCACCAGCAATTTCCCATTCTCC and Mtnr1b-wtR 5'-TCTTGCCTGAGGAAGGTCAGAATCC for *wt* (143 bp amplicon) and Mtnr1b-LacF 5'-ACTTGCTTTAAAAAACCTCCCACA and Mtnr1bR 5'-ATGGGTCCCTGGAAGTCACTCACC for *ki* (666 bp amplicon). PCR was performed for 35 cycles of 30 s at 95°C, 30 s at 55 °C, 1 min at 72°C using Taq polymerase (Euromedex). Wild type and recombinant mice were generated and housed in the Chronobiotron facility (UMS3415 CNRS-University of Strasbourg) as described above (1.5-18 months, 20-60g) with a 12:12-h light:dark cycle and with food and water *ad libitum*. During all experiments, all efforts were made to minimize the number of animals used. Experimental procedures were approved by the Animal Care and Use Committee of Institute of Cellular and Integrative Neurosciences, University of Strasbourg, France

Tissue processing;

Mice were euthanized during the light phase (9.00-12.00 a.m.) by CO2 inhalation. The animals were fixed by transcardiac perfusion with either 4% phosphate-buffered formaldehyde for LacZ enzymology or Periodate-Lysine-Paraformaldehyde (PLP) fixative for immunohistochemistry (IHC) and *in situ* hybridization (ISH) (53) The brains were removed from the skulls and post-fixed for 24 hours with 4% formaldehyde for LacZ staining or 12 hours in PLP fixative for IHC/ISH. Formaldehyde and PLP-fixed brains were cryoprotected in 30% sucrose and snap-frozen in isopentane chilled to -78°C with a dry ice-ethanol mix. Some PLP-fixed brains were dehydrated and embedded in polyethylene-glycol (PEG) for IHC and ISH according to Klosen (54). Brains were then processed either as free floating (LacZ staining or IHC) or PEG sections (IHC/ISH): serial 40 µm sections were cut on a cryotome and collected in PBS containing 0.02% sodium azide before either LacZ enzymology or IHC.

LacZ histoenzymological staining

The LacZ beta-galactosidase enzyme activity was visualized using the chromogenic substrate 5-bromo-4-chloro-3-indolyl- β-d-galactopyranoside (X-gal) (55). After washing the sections 3 times for 15 min each in LacZ wash buffer (PBS, 2 mM $MgCl_2$, 0.01% sodium deoxycholate, 0.02% Nonidet-P40) at room temperature, they were stained overnight at 37 °C with the X-gal development solution (5mM $K_4Fe(CN)_6$, 5 mM $K_3Fe(CN)_6$, and 1mg/ml X-gal in LacZ wash buffer). On the following day, the sections were washed for 3 times 5 min each in LacZ wash buffer and mounted on gelatinized slides. Slides were dehydrated by 5 min bath in 70%, 95%, and 100% (twice) ethanol, cleared in toluene (twice) and coverslipped with Eukitt medium.

Immunohistochemistry (IHC)

Immunohistochemistry was performed on free floating sections after a 30 min permeabilization with 0.3% Triton X-100 in PBS. For immunohistochemitry on PEG sections, the sections were subjected to an antigen reactivation procedure for 1 hour at 95°C in 10 mM Tris-Citrate buffer. For single label IHC, LacZ was detected using a chicken anti-LacZ antibody (ab9361, Abcam, UK), followed by a biotinylated donkey anti-chicken antibody (Jackson ImmunoResearch, PA, USA) and Neutravidin Peroxidase (ThermoFisher). Peroxidase activity was visualized with Diaminobenzidine as a chromogen. For sequential double label IHC, LacZ was detected with the chicken anti-LacZ antibody followed by a peroxidase conjugated donkey anti chicken antibody (Jackson ImmunoResearch, PA, USA) and diaminobenzidine development. The second immunostaining was then performed using biotinylated secondary antibodies (Jackson ImmunoResaech, PA, USA) and Neutravidin peroxidase (ThermoFisher), followed by visualization of peroxidase activity using tyramide signal amplification with fluorescent tyramides (54). Vasopressinergic neurons were visualized using a rabbit antiserum against Neurophysin 2 (Sigma N0744, St Quentin Fallavier, France). Vasoactive Intestinal Peptide (VIP) was detected using a rabbit antiserum against VIP (Viper, Netherlands, Institute for Brain Research, Amsterdam, Netherlands) and Calretinin using a monoclonal mouse antibody (clone 6B3, Swant, Marly, Switzerland)

Combined ISH with IHC

Combined non radioactive ISH and IHC was performed on PLP-fixed PEG sections. Riboprobes were transcribed from linearized plasmids in the presence of digoxigenin-labelled nucleotides in accordance with standard procedures. We used *Mus musculus* probes for Gastrin Releasing Peptide (GRP 763 bp of *Mus musculus* NM 175012.4), Corticotropin Releasing Hormone (CRH 999 bp of *Mus musculus* NM 205769.3) and Glutamate Decarboxylase 1 and 2 (GAD1 983 bp of *Mus musculus* NM 008077.5, GAD2 879bp of *Mus musculus* NM 008078.2). The length of the probes was confirmed by formaldehyde-3-(N-morpholino) propanesulphonic acid agarose gel electrophoresis and Northern blotting. The *in situ* hybridization was performed as reported previously (46). Briefly, polyethylene glycol sections were postfixed, digested for 30 min at 37°C with 0.5µg/ml Proteinase K (Roche) and acetylated twice for 10 min in 100 mM triethanolamine and 0.25% acetic anhydride. Hybridization was performed for 40 h at 60°C with 200 ng/ml labelled sense or antisense probes in 50% formamide, 5×SSC, 5×Denhardt's solution and 1 mg/ml salmon sperm DNA. Stringency rinses were performed for 6×10 min in 0.1×SSC at 72°C. Digoxigenin-labelled bound probes were detected with alkaline phosphatase-labelled anti-digoxigenin antibodies (Roche). Alkealine phosphatase activity was visualized using Nitroblue Tetrazolium (NBT) and 5-bromo-4-chloro-3-indolyl-phosphate (BCIP). The sections were then processed for LacZ IHC as described above using a peroxidase conjugated donkey anti-chicken antibody (Jackson ImmunoResearch, PA, USA) and fluorescent tyramides for the visualization of peroxidase activity (55).

Image acquisition and processing for visualization of double labelings

Micrographs were taken on a Leica DMRB microscope (Leica Microsystems, Rueil-Malmaison, France) equipped with an Olympus DP50 digital camera (Olympus France, Rungis, France). The images were then processed with Adobe Photoshop CS6 (Adobe Systems, Mountain View, CA, USA). Bright field images of diaminobenzidine IHC or NBT/BCIP ISH stains were converted to "virtual" fluorescence images by inverting the images to negative images. The colors in these negative images were then converted to either red or green to be combined with the fluorescence images of the second stain.

Results

Transgenic reporter mice

Sequencing of the LacZ transgene sequence confirmed that the LacZ coding sequence started at the original ATG start codon of both the MT1 (*Mtnr1a*) and MT2 (*Mtnr1b*) receptor sequence and ended a few bases after the original stop codons (Fig. 1). Thus all upstream and downstream regulatory elements were conserved. Only potential regulatory elements located in intron 1-2 of the MLT receptor genes were lost by this approach.

All the different mouse strains bearing heterozygous or homozygous combinations of the different constructs (*Mtnr1a*$^{+/+}$, *Mtnr1a*$^{+/ki}$, *Mtnr1a*$^{ki/ki}$, *Mtnr1b*$^{+/+}$, *Mtnr1b*$^{+/ki}$, *Mtnr1b*$^{ki/ki}$) generated in this study were viable and healthy with normal reproductive cycles. We verified that *Mtnr1a*$^{+/ki}$ F1 mice generated by breeding with the MLT-competent C3H strain also produced melatonin, by assaying melatonin concentrations during the night. These heterozygous F1 crosses had 179.27±24.42 (mean±s.e.m.) pg of melatonin per pineal at night, and 23.28±9.54 pg per pineal during the day, within the range of MLT concentrations observed in the C3H mouse strain. These *Mtnr1a*$^{+/ki}$ and *Mtnr1b*$^{+/ki}$ F1 C57/C3H mice developed and bred normally.

LacZ enzyme and immunocytochemical staining

X-Gal LacZ histochemical staining was visible as dots in almost all brain areas (Fig. 2, SI Table 1). When LacZ expression was visualized by immunohistochemistry, in some neurons labelling could be seen in the nucleus together with lighter cytoplasmic staining sometimes extending into the dendrites. Only a few neurons displayed LacZ immunostaining throughout their cell body (Fig. 2), but even in these neurons one or two strongly stained dot-like structures were visible (Fig 2D). A similar difference between the LacZ enzyme stain and immunostain has previously been described in a number of papers (52). The strongly stained dot-like structures are most likely high density lysosomal accumulations of the *E.coli* LacZ, appearing larger in enzyme–stained sections because of increased diffusion of the reaction product.

In all regions we investigated, both the LacZ enzyme stain and immunostain could be detected. We used the LacZ enzyme stain for mapping studies because of the better contrast with this method. For double labelling we used immunostaining because it was easier to combine with either neuronal markers or *in situ* hybridization.

Validation of the transgenic approach for MT1

To validate the transgenic reporter strategy and check for faithful expression patterns of LacZ under the control of the MLT receptor regulatory elements, we compared the MT1-LacZ transgene expression pattern with ^{125}I-iodomelatonin binding in the mouse as described by Liu et al. (39). A similar comparative approach for the MT2-LacZ transgene was not feasible because ^{125}I-iodomelatonin binding reflects uniquely MT1 receptor expression; since it is absent on tissue sections from the MT1 gene knock-out mice (39).

In MT1-LacZ mice, the strongest reporter expression was observed in cells of the *pars tuberalis* of the adenohypophysis (Figs. 3 and 5). Other strongly labeled structures were the suprachiasmatic nucleus (SCN), the paraventricular nucleus of the thalamus (PVT) and the paratenial thalamic nucleus (PT) (Fig. 3). The anterior hypothalamic area (AHA) adjacent to the SCN displayed slightly lighter staining than the previously mentioned structures (Fig. 3). This expression pattern, particularly in the anterior region of the PVT-PT complex and the SCN-AHA area, was perfectly coincident to the ^{125}I-iodomelatonin binding described by Liu et al. (39).

MT1 and MT2 expression mapping in the mouse brain (Table 1 and Fig 3)

We analyzed the brains of adult male and female C57BL/6J mice between 1-5 and 18 months of age in all genotypes; wild type, heterozygous and homozygous LacZ knock-in (MT1 or MT2 knockout). Furthermore, as the C57BL/6J mice do not produce MLT, we also analyzed the brains of F1 C57BL/6J x C3H mice to investigate the influence of MLT on its own receptor's expression. Only mice carrying the LacZ transgene showed either LacZ enzyme labeling or LacZ immunolabeling - as expected, both stains were completely absent from wild type mice. Furthermore, we did not see any obvious differences in either MT1-LacZ or MT2-LacZ expression pattern related to age, sex or presence of MLT in the F1 crosses with C3H mice. The only obvious difference was between heterozygous and homozygous LacZ knock-in animals, the latter showing stronger enzyme and antibody staining than the former (data not shown), revealing a gene dosage effect as previously shown for MT1 in mice (39).

Strong MT1-LacZ reporter expression could be detected in only a few-structures in the mouse brain: the SCN, the PT and the PVT. Below the median eminence, the *pars tuberalis* of the pituitary contained by far the strongest labeled cells (Fig. 3, Table 1). In the SCN, MT1-LacZ expressing cells were seen in all quadrants with an apparent higher density in the core region (Fig. 3). In the olfactory bulb, preoptic area and some subnuclei of the geniculate nucleus, the density of MT1-LacZ expressing neurons was lower but still generalized (Figs 2, 3, 4). Finally, isolated dispersed cells could be detected in a number of structures throughout the brain (SI Appendix). Of note, no MT1-LacZ expression was detected in the telencephalic cortex, and only very few faintly labelled cells could be seen in the hippocampus.

On the contrary, MT2-LacZ expression in the mouse brain was far more widespread (Fig. 3, Table 1). MT2-LacZ could be seen from the olfactory bulb down to the brain stem, with the notable exception of the *pars tuberalis*, where only MT1-LacZ was detected. The highest density of MT2-LacZ-expressing cells was seen in the Islets of Calleja, but many other structures also contained robustly labeled cells. In the SCN, MT2-LacZ-expressing cells were less dense than those expressing MT1-LacZ (Fig. 4). The intensity of MT2-LacZ-expressing cells surrounding the SCN was higher than that of MT1-LacZ. One of the highest densities of MT2-LacZ expressing cells was seen in the paraventricular nucleus of the hypothalamus PVN, where labeled cells were concentrated in the dorso-lateral part of this structure (Fig. 3). MT2-LacZ expression was also quite widespread in the basal forebrain, the bed nucleus of the stria terminalis and the amydaloid complex, and showed a layered appearance in the optic tectum (Fig. 3).

A major difference between MT1-LacZ and MT2-LacZ expression was the presence of MT2-LacZ in the telencephalic area, most notably in the hippocampus. The strongest MT2-LacZ expression in the neocortex was observed in layer 4 neurons of the somatosensory cortex. In motor areas, visual areas, auditory areas and cingulate cortex, the density of MT2-LacZ expressing cells was reduced, becoming virtually undetectable in associative areas and in the entorhinal cortex. In the piriform cortex, MT2-LacZ was present in layer 2 neurons (Fig. 3). The hippocampus presented a very interesting pattern with very strong staining in the pyramidal neurons of the CA2 region and complete absence from the CA1 and CA3 zones. MT2-LacZ expression could also be seen in the hypothalamus and thalamus. In the hypothalamus, three structures displayed a particularly high density of MT2-LacZ expressing cells: the PVN as previously mentioned, but also the arcuate nucleus and the most medial part of the medial tuberal nucleus (Fig. 5). Next to the rostral arcuate nucleus, a few MT2-LacZ expressing cells were located in the ependymal layer, and could be identified as tanycytes by immunocytochemistry (Fig. 5).

The thalamic expression pattern for MT1 and MT2 was quite interesting (Fig. 6). While MT1-LacZ expression was strong in the PVT, only very few cells expressed MT2-LacZ in this structure. MT2-LacZ staining was present in an arc-shaped area encompassing the centro-medial and centro-lateral thalamic nuclei. MT1-LacZ expression within this thalamic complex was more restricted. Another notable site of MT2-LacZ expression was the dorsal raphe nucleus (Fig. 7). In this structure, only a very few isolated cells expressed MT1-LacZ reporter whereas MT2-LacZ positive cells clearly delineated the boundaries of the central dorsal raphe nucleus. These cells were visualized both with enzyme histochemistry and immunohistochemistry for the LacZ protein. The distribution of the MT2-LacZ expressing cells is highly reminiscent of serotoninergic neurons as visualized by the presence of serotonin itself, tryptophan hydroxylase or the serotonin transporter (56).

Few structures contained both MT1-LacZ- and MT2-LacZ-expressing cells. When this was the case, the expression of MT1-LacZ was usually limited to a more discrete area within these structures (see central thalamic complex). Finally, only a few structures seemed to express comparable levels of the two MLT receptors, most notably the SCN, the mitral cell layer of the olfactory bulb, the subfornical organ and the median and ventro-median preoptic nuclei (Table 1).

MT1-LacZ expression in the SCN (Figs. 4 and 8)

In the SCN, whereas MT2-LacZ expression encompassed the entire region, MT1-LacZ expression was stronger and more restricted (Fig. 4), suggesting localization within a specific cell type. We tested the 3 classical markers of neuronal subpopulations of the SCN, arginine vasopressin (AVP), vasoactive intestinal peptide (VIP) and gastrin-releasing peptide (GRP) (Figs. 7 and 8). AVP did not co-distribute with MT1-LacZ, which was consistent with the general aspect of staining (Fig. 8A). On the other hand, double immunostaining for VIP and MT1-LacZ showed that a very few VIP neurons in the ventrolateral quadrant of the SCN also stained for MT1-LacZ (Fig. 8B). Double immunostaining for MT1-LacZ and GRP proved inconclusive, because the GRP antibody stained only fibers and not cell bodies. We therefore used non-radioactive *in situ* hybridization to visualize GRP cell bodies. Again, some GRP cells expressed the MT1-LacZ transgene, but constituted only a minority of GRP neurons (Fig. 8C). As we failed to identify the majority of MT1-LacZ neurons, we examined Calretinin, which in the mouse is a marker of SCN core cells similar to Calbindin in the Syrian hamster. Double immunostaining for MT1-LacZ and Calretinin showed all possible scenarios: Calretinin-positive/MT1-positive, Calretinin-positive/MT1-negative, and Calretinin-negative/MT1-positive cells (Fig. 8D). Therefore it appears that MT1-LacZ is expressed in a subpopulation of VIP neurons and some SCN core cells, but the majority of MT1-LacZ expressing SCN cells remain to be identified. We could exclude astrocytes, as a GFAP/MT1-LacZ stain did not show any co-localisation of these two markers.

MT2-LacZ expression in the paraventricular nucleus of the hypothalamus

Much like MT1-LacZ expression in the SCN, MT2-LacZ expression in the PVN was restricted to a subpopulation of PVN neurons. An AVP/MT2-LacZ double immunostain showed that MT2-LacZ was clearly not expressed either in the magnocellular or the parvocellular AVP neurons of the PVN (Fig. 9A). The MT2-LacZ expression pattern in the dorsolateral domain of the PVN suggested that the MT2-LacZ expressing cells might be CRH neurons (56). As for GRP in the SCN, immunostaining for CRH only stained the CRH fibers and not the cell bodies. Therefore, we stained CRH neurons by non-radioactive *in situ* hybridization for the CRH mRNA. In these double label studies, both CRH mRNA and MT2-LacZ immunolabel were clearly located in the medial parvicellular part of the dorsal PVN. In

some cells, MT2-LacZ was clearly co-localized with CRH, but there were also single labeled cells for either MT2-LacZ or CRH (Fig. 9B).

MT2-LacZ expression in the hippocampus (Fig. 10

The MT2-LacZ expression pattern in the hippocampus proved interesting in several aspects. First, while MT2-LacZ expression was clearly present in the hippocampus with strong immunostaining in some cells, MT1-LacZ expression appeared to be completely absent. Second, MT2-LacZ expression was present in two very distinct zones and two completely different neuronal types. Firstly, MT2-LacZ was expressed in the pyramidal cell layer of the CA2 but was completely absent from either CA1 or CA3 (Fig. 2, Fig. 10A). We identified GABAergic cells in the hippocampus by combining immunolabeling for MT2-LacZ with non-radioactive *in situ* hybridization for either GAD1 or GAD2. While we could find a few GABAergic interneurons also expressing MT2-LacZ, the vast majority of the MT2-LacZ expressing neurons in the CA2 contained neither GAD1 nor GAD2, and thus most probably constitute excitatory glutamatergic pyramidal neurons (Fig. 10B). In the hilus of the dentate gyrus, MT2-LacZ expression was also sometimes co-localized with GAD1 or GAD2 mRNA (Fig. 10C). Secondly, there was a population of small interneurons located mainly in the outer molecular layer of the dentate gyrus (Fig. 10A and D). This cell type was also seen in the most ventral parts of the subiculum and the outer layer 1 of the most ventral areas of the entorhinal cortex, the pyriform cortex and the cortical amygdalar areas. These were among the most strongly MT2-LacZ-stained cells, particularly within the cytoplasm. They were also one of the few cell types where immunostaining extended into the dendrites allowing clear visualization of the dendritic structure of these cells. Based on this staining, these cells were qualified as “small horizontal interneurons”. We were unable to find any description of similar cells in the literature, and our attempts to phenotype them were unsuccessful: we screened a large battery of neuropeptide antibodies and mRNA probes to look for staining in this population of MT2-LacZ neurons but were unable to find any neuropeptide marker that stained such “small horizontal interneurons”. Although the outer molecular layer contained some GABAergic neurons, most of these MT2-LacZ neurons expressed neither GAD1 nor GAD2 (Fig. 10E).

MT1- and MT2-LacZ expression in the retina (Fig. 11)

Both MT1-LacZ and MT2-LacZ expression were seen in the retina. Weak MT1-LacZ enzyme staining was detected in numerous photoreceptor inner segments, indicating the majority of labeled cells were rods (Fig. 11A). MT1-LacZ expression could also be detected in isolated cells located in the vitreal-most part of the inner nuclear layer (INL), likely a subset of amacrine cells, and in a few isolated cells in the ganglion cell layer (GCL) (Fig. 11A and C). MT2-LacZ expression was absent from the photoreceptor layer, but could be detected in some cells in the inner part of the INL and GCL (Fig. 11B and D). MT2-LacZ stained cells were more numerous than MT1-LacZ in these inner layers, but MT1-LacZ expression in putative amacrine cells was stronger than MT2-LacZ expression. Also, MT1-LacZ and MT2-LacZ expression was observed in distinctly separate subsets of amacrine cells: MT2-LacZ positive amacrine cells were smaller and located closer to the boundary of the inner nuclear and plexiform layers, whereas MT1-LacZ positive cells were more internally positioned within the INL. Furthermore, the strong MT1-LacZ immunostaining extended into their dendrites (Fig. 11E). These MT1-LacZ positive cells do not contain calretinin (Fig. 11F) and their dendrites ramified at the interface of strata S1 and S2 (Fig. 11F). In tyrosine hydroxylase - LacZ double immunostains, the dendrites of MT1-LacZ positive neurons clearly ramified below the layer of tyrosine hydroxylase-positive dendrites (Fig. 11G). We detected only a single cell double labeled for both MT1-LacZ and tyrosine hydroxylase in all the animals that we analyzed (Fig. 11H).

Discussion

The present "knock-in" strategy which replaces the MT1 or MT2 coding sequences with the LacZ reporter inserted into the endogenous loci has for the first time allowed to clearly differentiate cells/neurons containing MT1 and MT2 receptors in the mouse brain. Striking differences in the distribution of MT1 and MT2 receptors were observed. Compared with the MT1 subtype which was expressed in only a few structures, MT2 subtype receptors were identified in numerous brain structures. Targeted disruption of MT1 receptors results in the total disappearance of 2-iodomelatonin binding sites in the mouse brain, while such disappearance was not observed following disruption of MT2 receptors (39). It seems thus that in the mouse, the well described 2-iodomelatonin binding sites on tissue sections are exclusively due to binding to the MT1 receptor. The expression of MT2 has not been previously clearly detectable by *in situ* hybridization. Consequently, and contrary to the situation for MT1-LacZ, there are no experimental data to allow comparative validation of the present results for MT2. Nevertheless, independent validation of the results obtained with MT1-LacZ, and the fact that the MT2-LacZ knock-in was generated with an identical strategy, lead us to conclude that the LacZ staining faithfully reports MT2 expression as well. Notably, overlapping expression of the 2 receptor subtypes was observed in only very few structures (see Table 1). Moreover, even in these structures co-expression was rarely if ever present in the same individual neurons/cells, as exemplified within the SCN (Fig. 4) or retina (Fig. 11). This suggests that the two receptor subtypes are cell/neuron-specific for almost all brain structures. The difference in the distribution pattern of MT1 and MT2 receptors thus not only indicates the compartmentalization of several physiological functions by MLT, but also raises several fundamental questions about the mechanism of action of these receptors.

It has been suggested that MT1 and MT2 receptor subtypes form heterodimers *in situ* (58, 59,). However this heterodimerization, has only been demonstrated in *in vitro* studies. With the exception of the work of Baba et al (60) which used transgenic mice, full validation is lacking. An absolute minimal requirement for MT1/MT2 heterodimer formation is that they be expressed in the same cell/neuron. There are no clear data available from the literature to support such a heterodimer hypothesis. Thus, the *bona fide* presence of MT1/MT2 heterodimers in the brain and their physiological relevance remains a matter of debate.

It has also been reported that MLT receptors have the capacity to heterodimerize with other GPCRs (61). In this context the expression of MT2-LacZ in the dorsal raphe (Fig. 7) is of particular interest. The antidepressant effect of agomelatine (61) is considered to be due to the "synergistic" MLT agonist/5-HT2C antagonist profile of the drug. Heterodimerization of MT2 with serotonin receptor subtypes (5HT2C) might explain such data (62). The existence of functional MT2/5-HT2C heterodimers has been demonstrated but again only *in vitro* (63). In the present work the pattern of MT2-lacZ expression in the dorsal raphe is quite similar to the distribution of serotoninergic neurons but not that of GABAergic interneurons (64). Previous studies have demonstrated that 5HT2C-mediated negative feedback on serotoninergic neuron activity occurs through 5-HT2C receptors on GABAergic neurons of the dorsal raphe (65-67). The GABAergic neurons then inhibit the activity of the L-type voltage dependent calcium channels responsible for the spontaneous activity of serotoninergic neurons (68). Consequently, the cell type mediating the melatoninergic agonistic action of agomelatine appears to be distinct from the cell type responsible for the 5-HT2C antagonist action. Therefore in the dorsal raphe, MT2/5-HT2C heterodimerization is probably not an active phenomenon. Nevertheless, it might be present in some other brain structures. According to the Allen Mouse Brain reference Atlas (mouse brain-map.org), 5-HT2C containing neurons are present in layer 4 of the cortex, a structure which displays MT2-lacZ

staining. In the central thalamus (Fig. 6) and BNST (Fig. 3) the presence of both MT2 and 5-HT2C receptors might allow heterodimerization of these two receptors. Clearly, further studies are essential to address the exact role of receptor heterodimerization in the field of MLT biology.

The distinct distribution patterns of the two MLT receptor subtypes shown in the present work indicate that they may mediate different/divergent functions. Such functions will only be clearly distinguished once highly selective MT1 and MT2 agonists or antagonists are developed. Even if extensive work to develop such compounds has been performed in the last decades (36-38, 69-70), most of these ligands have weak selectivity which limits their use *in vivo,* meaning that current knowledge of the fundamental mechanisms involved is still very poor. Until now, MLT or MLT agonists beside action for the seasonal level have been mostly demonstrated to be useful in modulating clock (SCN) activity *in vivo* (chronobiotic effect, 71-73). MLT or drugs have proven effective in improving sleep latency, sleep efficiency and subjective total sleep time in individuals with perturbed sleep/wake cycles, as well as for non-24h sleep-wake disorders in blind people (74-77). Since these compounds (including authorized drugs, Agomelatine, Ramelteon, Tasimelteon and Circadin) are all non-specific MT1/MT2 agonists, they (as well as MLT) will act on both receptors when administered. The development of selective agonists to stimulate a given MLT receptor without affecting the other is thus necessary to understand the exact mechanism of action. As noted in the introduction, precise phenotyping of the neurons containing MLT receptor(s) is a prerequisite to understanding the physiological mechanisms involved. In the Siberian hamster which expresses only the MT1 subtype, receptors were observed in AVP-positive neurons of the SCN (47). We have not confirmed this observation in mice, but this may be due to species differences.

MLT does not work exclusively through action upon the SCN (chronobiotic effect). MLT has been described to affect almost all the main physiological functions of the body and to be useful in a vast array of experimental models reproducing different pathological conditions. Some of these observations are based on the use of pharmacological doses (1 mM and above) (78), as opposed to physiological doses (below the nanomolar range) (32). Looking at the large inter-species differences in the distribution of MLT binding sites in the brain (28-30) we cannot exclude that MLT acts very differently from one species to another (79).

Use of a "knock-in" strategy has allowed us to detect a large number of brain sites expressing the MT2 receptor gene. Interestingly, these structures have been described as containing MLT receptors in different mammalian species, even if the techniques used (e.g. immunocytochemistry) were not optimal. The precise identification of cells/neurons in these structures will open new perspectives for the identification of links between MLT brain targets and specific MLT receptor subtypes. For example, MLT receptors are expressed in key brain regions involved in memory (48). Co-expression of MT1 and MT2 in pyramidal neurons of the hippocampus (as shown by RT-PCR) (80) has been reported. Immunohistochemical analysis showed that MT1 and MT2 expression patterns partially overlap, with MT1 being expressed predominantly in the CA1 hippocampal subfield and MT2 in the CA3/CA4 subfields (48). Our present results allow unambiguous identification of MT2 expressing cells in the hippocampus, and apparent absence of MT1, and should facilitate experimental studies on the mechanism of MLT action on memory (81-86).

The moderate MLT receptor immunoreactivity in the rat dorsal raphe nucleus suggested the possible involvement of MT1 receptors in the pathogenesis of depression (48). This is supported by a study which demonstrated behavioral changes mimicking the symptoms of melancholic depression in MLT receptor knockout mice (87). There is evidence of MLT imposing tonic inhibitory control over a subpopulation of serotonin-containing

neurons in the dorsal raphe (87). Our study demonstrates a link between MLT and serotonin neurotransmission through MT2 receptors.

Finally the results obtained in the retina deserve some comments. Functional MLT receptors were first characterized in the retina (89), and immunohistochemical and *in situ* studies in rodent and human retina (90- 92) have shown that both receptors are detected in virtually every cell (93-95). This observation was used as strong evidence in favor of MLT receptor heterodimerization (96). The hypothetical physiological concept is that MLT secreted from photoreceptors (or from the general circulation) binds to MLT receptors on amacrine cells thereby inhibiting dopamine release, and conversely that dopamine binding to D2 receptors on photoreceptor cells suppresses MLT synthesis (97). MT1 receptors are detected in the photoreceptor layer, and both MT1 and MT2 receptors are present in scattered but distinct amacrine and ganglion cells. Our present data argue against heterodimerization of the two receptors, at least in mouse photoreceptors. Again, we will have to await further experimental work using specific agonists or antagonists in order to determine the mechanism of action of MLT within the retina. This line of reasoning can be extended to nearly all brain structures (see above and in the figures) identified in the present work.

In conclusion, the present work using a "knock-in" strategy has allowed us to determine fundamental differences in the distribution of MT1 and MT2 receptors in the mouse brain. The abundance of MT2 receptors was observed to be much greater than previously thought. Clearly, discovery of new pharmaco logical tools selective for each receptor subtype is critical for a clearer understanding of MLT action, and in order to develop innovative therapeutic approaches for pathologies such as diabetes, cancer, depression, memory failure, etc.

Acknowledgements

The authors are grateful to the Chronobiotron platform, UMS3415, CNRS, University of Strasbourg) for help with animals management. This work was supported by the Centre National de la Recherche Scientifique, University of Strasbourg (EC, DH, MPF, PK, PP and S Lapmaneya) and the Institut de Recherches Internationales Servier (CSK and BGL).

The authors have no potential conflict of interest with respect to the research, authorship, and/or publication of this article. Recombinant ES cells and the Mtnr1b$^{+/ki}$ mice were generated in the Knock Out Mouse Project (KOMP). The Mtnr1a$^{+/ki}$ strain was generated in the Institut Clinique de la Souris (Illkirch, France).

References

1. Schernhammer ES, Kroenke CH, (2006) Night work and risk of breast cancer. Epidemiology 17:108–111.

2. Dochi M, Suwazono Y, Sakata K, Okubo Y, Oishi M, Tanaka K, Kobayashi E, Nogawa K (2009) Shift work is a risk factor for increased total cholesterol level: a 14-year prospective cohort study in 6886 male workers. Occup Environ Med 66:592-597.

3. Bechtold DA, Gibbs JE, Loudon AS (2010) Circadian dysfunction in disease. Trends Pharmacol Sci 31:191–198.

4. Schroeder AM, Colwell CS (2013) How to fix a broken clock. Trends Pharmacol Sci 34:605–619.

5. Zelinski EL, Deibel SH, McDonald RJ (2014) The trouble with circadian clock dysfunction: multiple deleterious effects on the brain and body. Neurosci Biobehav Rev 40:80-101.

6. Barclay JL, Tsang AH, Oster H (2012) Interaction of central and peripheral clocks in physiological regulation. Prog Brain Res 199:163–181.
7. Dibner C, Schibler U, Albrecht U (2010) The mammalian circadian timing system: organization and coordination of central and peripheral clocks. Ann Rev Physiol 72:517–549.
8. Buijs RM, Kalsbeek A (2001) Hypothalamic integration of central and peripheral clocks. Nat Rev Neurosci 2:521–526.
9. Pevet P, Challet E (2011) Melatonin: both master clock output and internal time-giver in the circadian clocks network. J Physiol Paris 105:170–182.
10. Hardeland R, Cardinali DP, Srinivasan V, Spence DW, Brown GM, Pandi-Perumal S (2011) Melatonin--a pleiotropic, orchestrating regulator molecule. Prog Neurobiol 93:350-384.
11. Acuña-Castroviejo D, Escames G, Venegas C, Díaz-Casado ME, Lima-Cabello E, López LC, Rosales-Corral S, Tan DX, Reiter RJ (2014) .Extrapineal melatonin: sources, regulation, and potential functions. Cell Mol Life Sc 71:2997-3025.
12. Pevet P (2002) The melatonin. Dialogues Clin Neurosci 4:57–72.
13. Tosini G, Baba K, Hwang CK, Iuvone PM (2012) Melatonin: an underappreciated player in retinal physiology and pathophysiology. Exp Eye Res 103:82-89.
14. Perreau-Lenz S, Kalsbeek A, Van Der Vliet J, Pevet P, Buijs RM (2005). In vivo evidence for a controlled offset of melatonin synthesis at dawn by the suprachiasmatic nucleus in the rat. Neuroscience 130:797–803.
15. Arendt J (2005) Melatonin: characteristics, concerns, and prospects. J Biol Rhythms 20:291–303.
16. Reiter RJ 1993a) The melatonin rhythms: both a clock and a calendar. Experientia. 49:654-664.
17. Malpaux B, Tricoire H, Mailliet F, Daveau A, Migaud M, Skinner DC, Pelletier J, Chemineau P 2002) Melatonin and seasonal reproduction: understanding the neuroendocrine mechanisms using the sheep as a model. Reprod Suppl. 59:167-179
18. Pevet P (2003) Melatonin: from seasonal to circadian signal. J Neuroendocrinol 15:422-426.
19. Morgan PJ, Hazlerigg DG (2008) Photoperiodic signalling through the melatonin receptor turns full circle.. J Neuroendocrinol 20:820-826.
20. Revel FG, Masson-Pevet M, Pevet P, Mikkelsen JD, Simonneaux V (2009). Melatonin controls seasonal breeding by a network of hypothalamic targets. Neuroendocrinology. 90:1-14.
21. Barrett P, Bolborea M (2012) Molecular pathways involved in seasonal body weight and reproductive responses governed by melatonin. J Pineal Res 52:376-388.
22. Lerner AB, Case JD, Takahashi Y (1960) Isolation of melatonin and 5- methoxyindole-3-acetic acid from bovine pineal glands. J Biol Chem 235:1992–1997.
23. Benítez-King G (2006) Melatonin as a cytoskeletal modulator: implications for cell physiology and disease. J Pineal Res 40:1–9.
24 Boutin JA (2015) Quinone reductase 2 as a promising target of melatonin therapeutic actions. Expert Opin Ther Targets 20:1–15.
25. Galano A, Tan DX, Reiter RJ (2013) On the free radical scavenging activities of melatonin's metabolites AFMK and AMK. J Pineal res 54:245-525.
26. Ng KY, Leong MK, Liang H, Paxinos G (2017) Melatonin receptors: distribution in mammalian brain and their respective putative functions. Brain Struct Funct 222 :2921-2939.
27. Weaver DR, Rivkees SA, Reppert SM (1989) Localization and characterization of melatonin receptors in rodent brain by in vitro autoradiography. J Neurosci 9:2581-2590.

28. Masson-Pevet M, George D, Kalsbeek A, Saboureau M, Lakhdar-Ghazal N, Pevet P 1994) An attempt to correlate brain areas containing melatonin binding sites with rhythmic functions: a study in five hibernator species. Cell Tissue Res 278:97–106.
29. Maywood ES, Bittman EL, Ebling FJ, Barrett P, Morgan P, Hastings MH (1995) Regional distribution of iodomelatonin binding sites within the suprachiasmatic nucleus of the Syrian hamster and the Siberian hamster. J Neuroendocrinol 7:215–223.
30. Vanecek J, Pavlik A, Illnerova H (1987) Hypothalamic melatonin receptor sites revealed by autoradiography. Brain Res 435:359-362.
31. Reppert SM, Weaver DR, Ebisawa T (1994) Cloning and characterization of a mammalian melatonin receptor that mediates reproductive and circadian responses. Neuron 13:1177–1185.
32. Dubocovich ML, Delagrange P, Krause DN, Sugden D, Cardinali DP, Olcese J. (2010) International Union of Basic and Clinical Pharmacology. LXXV Nomenclature, classification, and pharmacology of G protein-coupled melatonin receptors. Pharmacol Rev 62:343–380. [
33. Jockers R, Delagrange P, Dubocovich ML, Markus MP, Nicolas Renault N, , Tosini GP, Cecon A, Zlotos DP. (2016) Update on melatonin receptors: IUPHAR Review 20 British Journal of Pharmacology 173 2702–2725.
34. Jockers R, Maurice P,. Boutin J, Delagrange P (2008) Melatonin receptors, heterodimerization, signal transduction and binding sites: What's new? Br. J. Pharmacol. 154, 1182–1195.
35. Legros C; Brasseur C; Delagrange P; Ducro P; Nosjean O; Boutin, J (2016). Alternative radioligands for investigating the molecular pharmacology of melatonin receptors. J. Pharmacol. Exp. Ther. 2016, 356, 681–692
36. Mor M.; Rivara S; Pala D; Bedini .; Spadoni G; Tarzia G (2010) Recent advances in the development of melatonin MT1 and MT2 receptor agonists. Expert Opin Ther Pat 20:1059–1077
37. Spadoni G, Bedini A, Lucarini S, Mari M, Caignard DH, Boutin JA, Delagrange P, Lucini V, Scaglione F, Lodola A, Zanardi F, Pala D, Mor M, Rivara S 2015) Highly Potent and Selective MT2 Melatonin Receptor Full Agonists from Conformational Analysis of 1-Benzyl-2-acylaminomethyl-tetrahydroquinolines. J Med Chem 58:7512-7525.
38. Rivara S, Pala D, Bedini A, Spadoni G (2015) Therapeutic uses of melatonin and melatonin derivatives: a patent review (2012 - 2014). Expert Opin Ther Pat 25:425-441.
39. Liu C, Weaver DR, Jin X, Shearman LP, Pieschl RL, Gribkoff VK, Reppert SM (1997) Molecular dissection of two distinct actions of melatonin on the suprachiasmatic circadian clock. Neuron 19:91-102.
40. Masana MI, Benloucif S, Dubocovitch Ml (2000). Circadian rhythm of mt1 melatonin receptor expression in the surprachiasmatic nucleus of the C3H/H/HeN mouse. J Pineal Res 28:185-192
41. Weaver DR, Reppert SM (1996) The Mel1a melatonin receptor gene is expressed in human suprochiasmatic nuclei. Neuroreport 8:109-112.
42. Soares JM Jr, Masana MI, Erşahin C, Dubocovich ML (2003) Functional melatonin receptors in rat ovaries at various stages of the estrous cycle. J Pharmacol Exp Ther 306:694-702
43. Uz T, Arslan AD, Kurtuncu M, Imbesi M, Akhisaroglu M, Dwivedi Y, Pandey GN, Manev H (2005) The regional and cellular expression profile of the melatonin receptor MT1 in the central dopaminergic system. Brain Res Mol Brain Res 136:45-53
44. Schuster C, Gauer F, Guerrero H, Lakhdar-Ghazal N, Pevet P, Masson-Pevet, M (2000) Photic regulation of mt1 melatonin receptors in the siberian hamster pars tuberalis and suprachiasmatic nuclei: Involvement of the circadian clock and intergeniculate leaflet. J. Neuroendocrinology, 12, 207-216.

45. Poirel VJ, Cailotto C, Streicher D, Pevet P, Masson-Pévet M, Gauer F (2003) MT1 melatonin receptor mRNA tissular localization by PCR amplification. Neuroendocrinology letter 24: 33-38:
46. Klosen P, Bienvenu C, Demarteau O, Dardente H, Guerrero H, Pevet P, Masson-Pévet M (2002) The mt1 melatonin receptor and RORbeta receptor are co-localized in specific TSH-immunoreactive cells in the pars tuberalis of the rat pituitary. J Histochem Cytoche50:1647–1657.
47. Song CK, Bartness TJ, Petersen SL, Bittman E, (2000). Co-expression of melatonin (MEL1a) receptor and arginine vasopressin mRNAs in the Siberian hamster suprachiasmatic nucleus. J Neuroendocrinol. 2000 Jul;12(7):627-34.
48. Lacoste B, Angeloni D, Dominguez-Lopez S, Calderoni S, Mauro A, Fraschini F, Descarries L, Gobbi G (2015) Anatomical and cellular localization of melatonin MT1 and MT2 receptors in the adult rat brain. J Pineal Res 58:397-417.
49. Waly N E, Hallworth R (2015) Circadian Pattern of Melatonin MT1 and MT2 Receptor Localization in the Rat Suprachiasmatic Nucleus. Journal of Circadian Rhythms, 13:1-7.
50. Adamah-Biassi EB, Zhang Y, Jung H, Vissapragada S, Miller RJ, Dubocovich Ml (2014) Distribution ofMT1melatonin receptor promoter-driven RFP expression in the brains of BAC C3H/HeN transgenic mice. J Histochem Cytochem 62:70–84.
51. Valenzuela DM, Murphy AJ, Frendewey D, Gale NW, Economides AN, Auerbach W, Poueymirou WT, Adams NC, Rojas J, Yasenchak J, Chernomorsky R, Boucher M, Elsasser AL, Esau L, Zheng J, Griffiths JA, Wang X, Su H, Xue Y, Dominguez MG, Noguera I, Torres R, Macdonald LE, Stewart AF, DeChiara TM, Yancopoulos GD (2003) High-throughput engineering of the mouse genome coupled with high-resolution expression analysis Nat Biotechnol 21:652-659.
52 Mattapallil MJ, Wawrousek EF, Chan CC, Zhao H, Roychoudhury J, Ferguson TA, Caspi RR 2012) The Rd8 mutation of the Crb1 gene is present in vendor lines of C57BL/6N mice and embryonic stem cells, and confounds ocular induced mutant phenotypes. Invest Ophthalmol Vis Sci 53:2921-2937.
53. Sekerková G, Katarova Z, Joó F, Wolff JR, Prodan S, Szabó G (1997) Visualization of beta-galactosidase by enzyme and immunohistochemistry in the olfactory bulb of transgenic mice carrying the LacZ transgene.J Histochem Cytochem 45:1147-1155.
54. Klosen P, Maessen X, van den Bosch de Aguilar P (1993). PEG embedding for immunocytochemistry: application to the analysis of immunoreactivity loss during histological processing. J Histochem Cytochem 41:455-463.
55 Hopman AH, Ramaekers FC, Speel EJ (1998) Rapid synthesis of biotin-, digixigenin-, trinitrophenyl-, and flurochrome-labeled tyramides and their application for *In situ* hybridization using CARD application. J Histochem Cytochem 46:771-777.
56. Dougherty JD, Maloney SE, Wozniak DF, Rieger MA, Sonnenblick L, Coppola G, Mahieu NG, Zhang J, Cai J, Patti GJ, Abrahams BS, Geschwind DH, Heintz N (2013) The disruption of Celf6, a gene identified by translational profiling of serotonergic neurons, results in autism-related behaviors. J Neurosci 33: 2732-2753
57. Biag J, Huang Y, Gou L, Hintiryan H, Askarinam A, Hahn JD, Toga AW, Dong HW (2012) Cyto- and chemoarchitecture of the hypothalamic paraventricular nucleus in the C57BL/6J male mouse: a study of immunostaining and multiple fluorescent tract tracing. J Comp Neurol. 520:6-33.
58. Levoye A; Jockers R; Ayoub M.A. Delagrange P; Savaskan E; Guillaume J L (2006) Are G protein-coupled receptor heterodimers of physiological relevance? Focus on melatonin receptors. Chronobiol Int 23, 419−426

59. Zlotos D.P; Jockers R; Cecon E; Rivara S, Witt-Enderby PA (2014) MT1 and MT2 melatonin receptors: Ligands, models, oligomers, and therapeutic potential. J Med Chem 57:3161–3185.
60 Baba K, Benleulmi-Chaachoua A, Journé AS, Kamal M, Guillaume JL, Dussaud S, Gbahou F, Yettou K, Liu C, Contreras-Alcantara S, Jockers R, Tosini G (2013) Heteromeric MT1/MT2 melatonin receptors modulate photoreceptor function. Sci Signal. 2013 Oct 8;6(296):ra89. doi: 10.1126/scisignal.2004302.
61. De Bodinat C, Guardiola-Lemaitre B, Mocaer E, Renard P, Munoz C, Millan M.J (2010) Agomelatine, the first melatonergic antidepressant: Discovery, characterization and development. Nat Rev Drug Discov 9, 628–642. [
62. Kamal M, Gbahou F, Guillaume JL, Daulat AM, Benleulmi-Chaachoua A, Luka M, Chen P, Kalbasi Anaraki D, Baroncini M, Mannoury la Cour C, Millan MJ, Prevot V, Delagrange P, Jockers R (2015) Convergence of melatonin and serotonin (5-HT) signaling at MT2/5-HT2C receptor heteromers. Journal of Biological Chemistry 290:11537-11546
63. Ayoub MA, Couturier C, Lucas-Meunier E, Angers S, Fossier P, Bouvier M, Jockers R (2002) Monitoring of ligand-independent dimerization and ligand-induced conformational changes of melatonin receptors in living cells by bioluminescence resonance energy transfer. J. Biol. Chem. 277: 21522–21528.
64. Gocho Y, Sakai A, Yanagawa Y, Suzuki H, Saitow F (2013) Electrophysiological and pharmacological properties of GABAergic cells in the dorsal raphe nucleus. Journal of Physiological Science 63: 147-154.
65. Serrats J, Mengod G. Cortés R (2005) Expression of serotonin 5-HT2C receptors in GABAergic cells of the anterior raphe nuclei. J Chem Neuroanat 29:83-91.
66. Quérée P., Peters S. & Sharp T. (2009) Further pharmacological characterization of 5-HT(2C) receptor agonist-induced inhibition of 5-HT neuronal activity in the dorsal raphe nucleus in vivo. British Journal of Pharmacology 158: 1477-1485
67. Boothman L, Raley J, Denk F, Hirani E, Sharp T (2006) In vivo evidence that 5-HT(2C) receptors inhibit 5-HT neuronal activity via a GABAergic mechanism. British Journal of Pharmacology 149: 861-869
68. Asaoka N, Nishitani N, Kinoshita H, Kawai H, Shibui N, Nagayasu K, Shirakawa H, Nakagawa T, Kaneko S (2017) Chronic antidepressant potentiates spontaneous activity of dorsal raphe serotonergic neurons by decreasing GABAB receptor-mediated inhibition of L-type calcium channels. Scientific Reports 7: 13609
69. Dubocovich ML, Masana MI, Iacob S, Sauri DM (1997) Melatonin receptor antagonists that differentiate between the human Mel1a and Mel1b recombinant subtypes are used to assess the pharmacological profile of the rabbit retina ML1 presynaptic heteroreceptor. Naunyn Schmiedebergs Arch Pharmacol 355:365–375.
70. Zlotos DP (2012) Recent progress in the development of agonists and antagonists for melatonin receptors. Curr. Med. Chem 19:3532–3549.
71. Arendt J, Skene DJ (2005) Melatonin as a chronobiotic Sleep Med Rev 9:25–39.
72. Pevet P; Bothorel, B., Slotten H, Saboureau M (2002) The chronobiotic properties of melatonin. Cell Tissue Res 309:183–191.
73. Pevet P (2016) Melatonin receptors as therapeutic targets in the suprachiasmatic nucleus. Exper Opin Ther Targets 20:1209-1218.
74. Emens JS, Burgess HJ (2015) Effect of light and melatonin and other melatonin receptor agonists on human circadian physiology. Sleep Med Clin 10:435–453.
75. Skene DJ, Arendt J (2007) Circadian rhythms disorders in the blind and their treatment with melatonin Sleep Med 8:651-655.

76. Lockley SW, Dijk DJ, Kosti O, Skene DJ, Arendt J (2008) Alertness, mood and performance rhythm disturbances associated with circadian sleep disorders in the blind. J Sleep Res17:207-216.
77. Fitzgerald LR, Reed JE (2004) Melatonin agonists for the treatment of sleep disorders and major depression. Ann Rep Med Chem 39: 25–37.
78. Reiter RJ, Tan DX, Rosales-Corral S, Manchester LC (2013) The universal nature, unequal distribution and antioxidant functions of melatonin and its derivatives. Mini Rev Med Chem 13:373–384.
79. Liu J, Clough SJ, Hutchinson AJ, Adamah-Biassi EB, Popovska-Gorevski M, Dubocovich ML (2016) MT1 and MT2 Melatonin Receptors: A Therapeutic Perspective. Annu Rev Pharmacol Toxicol 56:361-383.
80. Musshoff U, Riewenherm D, Berger E, Fauteck JD, Speckmann EJ (2002) Melatonin receptors in rat hippocampus: molecular and functional investigations. Hippocampus. 12:165-173.
81. Savaskan E, Ayoub MA, Ravid R, Angeloni D, Fraschini F, Meier F, Eckert A, Müller-Spahn F, Jockers R (2005) Reduced hippocampal MT2 melatonin receptor expression in Alzheimer's disease. J Pineal Res 38:10-16.
82. Wang LM, Suthana NA, Chaudhury D, Weaver DR, Colwell CS (2005) Melatonin inhibits hippocampal long-term potentiation. Eur J Neurosci 222 231-237.
83. Collins DR, Davies SN (1997) Melatonin blocks the induction of long-term potentiation in an N-methyl-D-aspartate independent manner. Brain Res 29:767(1):162-165.
84. El-Sherif Y, Witt-Enderby P, Kai Lid P, Jene Tesoriero J, Hogan MV, Wieraszko A (2004) The actions of a charged melatonin receptor ligand, TMEPI, and an irreversible MT2 receptor agonist, BMNEP, on mouse hippocampal evoked potentials in vitro. Life Sci. 75, 3147–3156
85. Larson J, Jessen RE, Uz T, Arslan AD, Kurtuncu M, Imbesi M, Manev H (2006) Impaired hippocampal long-term potentiation in melatonin MT2 receptor-deficient mice. Neurosci Lett 393:23-26.
86. Jilg A, Bechstein P, Saade A, Dick M, Li TX, Tosini G, Rami A, Zemmar A, Stehle JH. Melatonin modulates daytime-dependent synaptic plasticity and learning efficiency. J Pineal Res. 2019 Jan 7:e12553. doi: 10.1111/jpi.12553.
87. Comai S, Ochoa-Sanchez R, Dominguez-Lopez S, Bambico FR, Gobbi G (2015) Melancholic-Like behaviors and circadian neurobiological abnormalities in melatonin MT1 receptor knockout mice. Int J Neuropsychopharmacol 18. 1-10 doi:10.1093/ijnp/pyu075
88. Domínguez-López S, Howell R, Gobbi G 2012) Characterization of serotonin neurotransmission in knockout mice: implications for major depression. Rev Neurosci 23:429-543.
89. Dubocovich ML (1984) Melatonin is a potent modulator of dopamine release in the retina. Nature.306 :782-784.
90. Fujieda H, Hamadanizadeh SA, Wankiewicz E, Pang SF, Brown GM (1999) Expression of mt1 melatonin receptor in rat retina: evidence for multiple cell targets for melatonin. Neuroscience. 93:793-799.
91. Scher J, Wankiewicz E, Brown GM, Fujieda H (2003) AII amacrine cells express the MT1 melatonin receptor in human and macaque retina. Exp Eye Res 77:375-382.
92. Savaskan E, Jockers R, Ayoub M, Angeloni D, Fraschini F, Flammer J, Eckert A, Müller-Spahn F, Meyer P (2007) The MT2 melatonin receptor subtype is present in human retina and decreases in Alzheimer's disease. Curr Alzheimer Res 4:47-51.
93. Yang XF, Miao Y, Ping Y, Wu HJ, Yang XL, Wang Z (2011) Melatonin inhibits tetraethylammonium-sensitive potassium channels of rod ON type bipolar cells via MT2 receptors in rat retina. Neuroscience 173:19-29.

94. Reppert SM, Godson C, Mahle CD, Weaver DR, Slaugenhaupt SA, Gusella JF (1995) Molecular characterization of a second melatonin receptor expressed in human retina and brain: the Mel1b melatonin receptor. Proc Natl Acad Sci U S A. 92:8734-8738.
95. Pack W, Hill DD, Wong KY (2015) Melatonin modulates M4-type ganglion-cell photoreceptors. Neuroscience 303:178-188.
96. Piano I, Baba K, Gargini C, Tosini G 2018) Heteromeric MT_1/MT_2 melatonin receptors modulate the scotopic electroretinogram via PKCζ in mice. Exp Eye Res 177:50-54.
97. Fujieda H, Scher J, Hamadanizadeh SA, Wankiewicz E, Pang SF, Brown GM. (2000) Dopaminergic and GABAergic amacrine cells are direct targets of melatonin: immunocytochemical study of mt1 melatonin receptor in guinea pig retina. 17:63-70.

Figure Legends

Figure 1. Targeting strategy for the generation of *Mtnr1a* and *Mtnr1b LacZ* knock in mice: the wild-type allele is representative of *Mtnr1a* gene but exon/intron structure and strategy are similar for *Mtnr1b*. A reporter-selection cassette containing a a) LacZ open reading frame, poly-A site and b) a floxed human Ubiquitin promoter, Neomycine resistance gene, poly-A site sequence, was inserted between the ATG and the stop codon region of the target gene by using a BAC strategy. Mice carrying this targeted allele were generated by ES cell-based/germline transmission. The final knock in mice were derived from the preceding ones by breeding with CRE-deleter mice to remove the selection gene and final segregation of the *Cre* gene.

Figure 2. MT1-LacZ expression in the suprachiasmatic nucleus detected by LacZ enzyme histochemistry (A, C) or by LacZ immunohistochemistry (B,D). The LacZ enzyme activity is visualized as strongly stained dots, which most probably are lysosomal accumulations of the transgenic LacZ enzyme (A,C). Immunohistochemical detection of the LacZ protein visualizes LacZ in these same dot-like structures, as well as in the nucleus and cytoplasm of most SCN neurons (B,D). The dot-like structures are bigger in enzyme histochemistry than in immunohistochemistry probably because of the higher diffusion of the X-Gal reaction product compared to the peroxidase diaminobenzidine precipitate.
MT1-LacZ expressing neurons are unevenly distributed in the SCN, with the highest density of MT1-LacZ expressing cells located in the medio-ventral quadrant of the SCN.
Bar in A = 100 µm for A/C, Bar = 50 µm for B/D

Figure 3. Mapping of MT1-LacZ and MT2-LacZ expression in the mouse brain. Comparable levels are shown for both MT1-LacZ and MT2-LacZ. While MT1-LacZ expression is reduced to only a few discrete structures (most notably the SCN, the PVT-PT complex, the SG and the *pars tuberalis*), MT2-LacZ expression is much more widespread, particularly in the forebrain.

Figure 4. MT1-LacZ (A) and MT2-LacZ (B) expression in the SCN. MT1-LacZ expression in the SCN is higher than MT2-LacZ expression and delineates the boundaries of the SCN. Furthermore, MT2-LacZ expression also is more diffuse in the anterior hypothalamic area.
Bar = 50 µm

Figure 5. MT1-LacZ (A) and MT2-LacZ (B,C) expression in the mediobasal hypothalamus.
The *pars tuberalis* of the adenohypophysis displays very high levels of MT1-LacZ expression. Furthermore, MT1-LacZ can be detected in some cells of the arcuate nucleus ((black arrow) and the medial tuberal nucleus (open arrow) particularly in the most rostral

regions of these structures (A). MT2-LacZ expression in the mediobasal hypothalamus is much more widespread than MT1-LacZ expression (B), with the notable exception of *the pars tuberalis,* which is completely devoid of MT2-LacZ staining (double arrow heads). As with all structures where both MT1-LacZ and MT2-LacZ expression can be detected, MT1-LacZ expression is present in a more reduced and discrete subset of cells than MT2-LacZ, as seen here for both the arcuate nucleus and the medial tuberal nucleus. MT2-LacZ expression is also detected in some cells of the ependymal wall, which are identified as tanycytes (arrowheads in C) in LacZ immunohistochemical staining by the processes (C).
Bar in B = 200 µm for A/B
Bar in C = 100 µm

Figure 6. MT1-LacZ and MT2-LacZ expression in the thalamus.
Both MT1-LacZ and MT2-LacZ expression can be seen in various nuclei of the central and dorsal thalamus, as well as the habenula (*). In the paraventricular nucleus of the thalamus, MT1-LacZ expression is particularly high (black arrowhead), while MT2-LacZ expression is reduced to a few cells. (open arrowhead). In almost all other structures, MT1-LacZ expression is reduced to a much smaller subset of cells than MT2-LacZ expression. In the habenula (*), almost no MT1-LacZ expression can be seen.
Bar = 250 µm

Figure 7. MT2-LacZ expression in the dorsal raphe nucleus by LacZ enzyme histochemistry (A, B) or immunohistochemistry (C). MT2-LacZ expression can be seen in cells delineating an inverted triangular area in the most central part of the dorsal raphe, similar to that observed for serotonergic neurons.
Bar = 100 µm

Figure 8. Colocalization of MT1-LacZ immunohistochemistry with neuropeptide markers in the suprachiasmatic nucleus.
(A) Double immunostaining for vasopressin-neurophysin2 (red) and MT1-LacZ (green) show no colocalisation.
(B) Colocalization of vasoactive intestinal peptide (red) and MT1-LacZ (green) in some cells in the most ventral part of the SCN (arrowheads).
(C) In the central part of the SCN, MT1-LacZ (green) can also be seen in some neurons expressing the mRNA for gastrin releasing peptide (red, non-radioactive in situ hybridization). After in situ hybridization, the LacZ immunostaining can only be seen in the dot like structures (arrowheads).
(D) In the central part of the SCN, calretinin (red) can be seen in a number of MT1-LacZ (green) expressing cells (arrowheads). However, there are also cells expressing only either calretinin (red) or MT1-LacZ (green).
Bar in D = 50 µm for A, B and D
Bar in C = 20 µm

Figure 9. Colocalization of MT2-LacZ immunohistochemistry with neuropeptide markers in the paraventricular nucleus of the hypothalamus.
(A) Double immunostaining for vasopressin-neurophysin2 (red) and MT2-LacZ (green) show no colocalisation. MT2-LacZ expression is present in cells located in the dorsal part of the medial parvicellular subdivision of the paraventricular nucleus.
(B) Double staining for MT2-LacZ (green) and the mRNA of corticotropin releasing hormone (CRH, red) shows that the MT2-LacZ neurons are mostly CRH neurons, although some MT2-

LacZ cells are clearly outside of the CRH neurons zone and some CRH neurons do not contain the green dot staining of MT2-LacZ.
Bar in A = 100 µm
Bar in B = 50 µm (insert bar = 20 µm)

Figure 10. MT2-LacZ expression in the hippocampus.
(A) Particularly dense MT2-LacZ dot-like immunostaining is seen in the CA2 region of the hippocampus (rectangle B). In the hilus of the dentate gyrus, (rectangle C) some lightly stained neurons are present. The strongest staining for MT2-LacZ however is detected in small neurons located in the outer molecular layer of the dentate gyrus (rectangle D). The rectangles show the areas selected for figures 9B, C and D.
(B) Only a few MT2-LacZ positive neurons in the CA2 area co localize with GAD1 or GAD2.
(C) In the hilus of the dentate gyrus, GAD1 or GAD2 can be detected in MT2-LacZ positive neurons (arrowheads).
(D) The small neurons located in the outer molecular layer of the dentate gyrus display a particularly strong immunostaining for LacZ, extending into their neurites.
(E) The MT2-LacZ positive neurons in the outer molecular layer mostly did not express either GAD1 or GAD2.
Bar in A = 250 µm
Bar in B = 50 µm for B, D and E
Bar in C = 25 µm

Figure 11. MT1-LacZ and MT2-LacZ expression in the retina. The pink staining of the nuclei is an inverted DAOI stain.
(A) Weak MT1-LacZ enzyme histochemical stain can be seen in the photoreceptor layer (PR). Much stronger enzyme activity is detected in some amacrine cells (fleche SVP) in the inner nuclear layer (INL) and some ganglion cells.(GCL).
(B) MT2-LacZ expression is absent from the photoreceptor layer, but present in some amacrine cells and some ganglion cells.
(C) MT1-LacZ expression in amacrine cells and ganglion cells. The cell bodies of the amacrine cells expressing MT1-LacZ are located within the inner nuclear layer (INL) away from the boundary of the inner nuclear layer with the inner plexiform layer (IPL).
(D) The cell bodies MT2-LacZ positive amacrine cells are mostly located at the interface between the inner nuclear and plexiform layers.
(E) In the MT1-LacZ amacrine cells, the LacZ immunostaining extends into a neurite ramifying in the upper strata of the inner plexiform layer.
(F) Double immunostaining for MT1-LacZ (red) and calretinin (green) shows that the MT1-LacZ amacrine cells are calretinin negative, and that their neurite ramifies in the upper calretinin layer between strata 1 and 2
(G) Most MT1-LacZ (green) amacrine cells are located higher than the dopaminergic amacrine cells (red, tyrosine hydroxylase).
(H) Only one MT1-LacZ cell (green) colocalized with tyrosine hydroxylase (red) identified
Bar in A = 50 µm for A and C
Bar in B = 20 µm for all other micrographs
PR photoreceptor layer, ONI outer nuclear layer, OPL outer plexiform layer, INL, Inner nuclear layer, IPL, inner plexiform layer, GCL, ganglion cell layer.

Table 1:

Mapping of MT1-LacZ and MT2-LacZ in the mouse brain. Abbreviations of the structures according to Franklin & Paxinos (2007) The Mouse Brain in Stereotaxic Coordinates Third Edition. Elsevier.

~	scattered isolated lightly labelled cells
±	scattered lightly labelled cells
+	scattered cells not delineating the structure
++	labelled cells delineating the structure
+++	high density of labelled cells
++++	very high density of labelled cells completely filling the structure

Contributions of each author

P. Klosen, Participate to the experimentation, analyse of the data and participate to the redaction

S Lapmanne participate to the experiment

C Schuster, participate to the analysis of the data

B Guardiola : participate to the analysis of the data

D Hicks: participate to the analyse of the data and participate to the redaction of the article

P. Pevet Participate to the design of the experiment, analyse the data and participate to the redaction of the article

MP Felder. Participate to the design to the experiment, to the experimental work, analyse the data and was responsible for the redaction of the article

Olfactory bulb, glomerular layer	OB gl
Olfactory bulb, mitral cell layer	OB mit
Accessory olfactory bulb, glomerular layer	AOB gl
Accessory olfactory bulb, mitral cell layer	AOB mit
Anterior olfactory nuclei	AO
Nucleus accumbens, shell	AcbSh
Ventral Pallidum	VP
Islets of Calleja	ICj
Caudate Putamen	CPu
Piriform cortex	Pir
Olfactory tubercle	Tu
Dorsal peduncular cortex	DP
Induseum griseum	IG
Diagonal band of Broca	VDB/HDB
Medial septal nucleus	MS
Median preoptic nucleus	MnPO
Organum vasculosum lamina terminalis	OVLT
Anteroventral periventricular nucleus	AVPe
Periventricular hypothalamic nucleus	Pe
Bed nucleus of the stria terminalis, rostral	BNSTr
Bed nucleus of the stria terminalis, caudal	BNSTc
Lateral septal nucleus, dorsal part	LSD
Lateral septal nucleus, intermediate part	LSI
Lateral septal nucleus, ventral part	LSV
Septofimbrial nucleus	Sfi
Triangular septal nucleus	TS
Subfornical organ	SFO
Ventromedial preoptic nucleus	VMPO
Medial preoptic area	MPA
Medial preoptic nucleus, medial part	MPOM
Lateral preoptic nucleus	LPO
Substantia innominata	SI
Suprachiasmatic nucleus	SCN
Paraventricular nucleus of the thalamus	PVT
Paratenial nucleus of the thalamus	PT
Mediodorsal thalamic nucleus	MD
Anterior hypothalamic area	AHA
Lateral hypothalamic area	LHA
Xiphoid & paraxyphoid thalamic nucleus	Xi/PaXi
Paraventricular nucleus of the hypothalamus, magnocellular	PVNmc
Paraventricular nucleus of the hypothalamus, parvocellular	PVNpc
Lateroanterior hypothalamic nucleus	LA
Posterior hypothalamic nucleus	PH
Ventromedial nucleus of the hypothalamus	VMH
Dorsomedial nucleus of the hypothalamus	DMH
Arcuate nucleus	Arc
RFRP-like	RFRP
Medial tuberal nucleus	Mtu
Peduncular part of lateral hypothalamus	PLH

Basomedial amygdaloid nucleus	BMA
Basolateral amygdaloid nucleus	BLA
Dentate gyrus, hilus	DGh
Dentate gyrus, granular layer	DGg
Dentate gyrus, molecular layer	DGm
CA2 field of the hippocampus	CA2
CA3 field of the hippocampus	CA3
Reuniens thalamic nucleus	Re
Central medial thalamic nucleus	CM
Paracentral thalamic nucleus	PC
Centrolateral thalamic nucleus	CL
Medial habenula	MHb
Lateral habenula	LHb
Intermediodorsal thalamic nucleus	IMD
Parafascicular thalamic nucleus	PF
Interanteromedial thalamic nucleus	IAM
Ventromedial thalamic nucleus	VM
Ventral posterolateral thalamic nucleus	VPL
Ventral posteromedial nucleus	VPM
Reticular nucleus	Rt
Dorsal lateral geniculate nucleus	DLG
Intramedullary thalamic nucleus	IMA
Pregeniculate nucleus	PG
Intergeniculate leaflet	IGL
Suprageniculate thalamic nucleus	SG
Medial geniculate nucleus medial part	MGM
Medial geniculate nucleus dorsal part	MGD
Peripeduncular nucleus	PP
Zona incerta	ZI
Red nucleus parvicellular part	RPC
Red nucleus magnocellular part	RMC
Substantia nigra pars compacta	SNC
Medial mammillary nucleus	MM
Retromammillary nucleus	RM
Subbrachial nucleus	SubB
Superficial gray superior colliculus	SUG
Intermediate gray superior colliculus	ING
Deep gray superior colliculus	DPG
Interpeduncular nucleus	IP
Interpeduncular nucleus, intermediate subnucleus	IPI
Dorsomedial periaqueductal gray	DMPAG
Lateral periaqueductal gray	LPAG
Ventrolateral periaqueductal gray	VLPAG
Dorsal raphe	DR
Median raphe	MnR
Medial accessory oculomotor nucleus	MA3
Dorsal nucleus of the lateral lemniscus	DLL
Reticulotegmental nucleus of the pons	RtTg
Pontine nuclei	Pn
External cortex of the inferior colliculus	ECIC

Nucleus brachium of the inferior colliculus	BIC
Parabrachial nucleus	PBN
Locus Coeruleus	LC
Dorsal cochlear nucleus	DC
Superior vestibular nucleus	SuVe
Medial vestibular nucleus	Mve
Medial longitudinal fascicle	mlf
Central gray	CG
Prepositus nucleus	Pr
Principal sensory trigeminal nucleus	Pr5
Spinal trigeminal nucleus	Sp5
Acessory nuclei of the abducens and facial nerve	Acs6/7
Raphe magnus nucleus	RMg
Area postrema	AP

		MT1	MT2
Telencephalon (Forebrain)			
Olfactory bulb, glomerular layer	OB gl		++
Olfactory bulb, mitral cell layer	OB mit		++
Accessory olfactory bulb, glomerular layer	AOB gl		++
Accessory olfactory bulb, mitral cell layer	AOB mit	++	++
Anterior olfactory nuclei	AO		+++
Olfactory tubercle	Tu		+
Nucleus accumbens, shell	AcbSh		++
Ventral Pallidum	VP		++
Islets of Calleja	ICj		++++
Caudate Putamen	CPu		±
Diagonal band of Broca	VDB/HDB		+±
Medial septal nucleus	MS		±
Basomedial amygdaloid nucleus	BMA	±	++
Basolateral amygdaloid nucleus	BLA		+
Substantia innominata	SI		+±
Lateral septal nucleus, dorsal part	LSD		++
Lateral septal nucleus, intermediate part	LSI		+±
Lateral septal nucleus, ventral part	LSV	+	++
Septofimbrial nucleus	Sfi		++
Triangular septal nucleus	TS		±
Subfornical organ	SFO	+±	++
Telencephalon (Cortex)			
Piriform cortex	Pir		++
Dorsal peduncular cortex	DP		+++
Induseum griseum	IG		+++
Telencephalon (Hippocampus)			
Dentate gyrus, hilus	DGh	~	±
Dentate gyrus, molecular layer	DGm		+
CA2 field of the hippocampus	CA2		++
CA3 field of the hippocampus	CA3	~	±
Diencephalon (Hypothalamus)			
Medial preoptic area	MPA		+
Median preoptic nucleus	MnPO	+±	++±
Organum vasculosum lamina terminalis	OVLT	+	+
Anteroventral periventricular nucleus	AVPe	+	++±
Lateral preoptic nucleus	LPO		+
Ventromedial preoptic nucleus	VMPO	++	++
Periventricular hypothalamic nucleus	Pe	±	++
Medial preoptic nucleus, medial part	MPOM		±
Bed nucleus of the stria terminalis, rostral	BNSTr	~	++
Bed nucleus of the stria terminalis, caudal	BNSTc		+
Suprachiasmatic nucleus	SCN	+++	++
Paraventricular nucleus of the hypothalamus, parvocellular	PVNpc		+++
Paraventricular nucleus of the hypothalamus, magnocellular	PVNmc		+
Anterior hypothalamic area	AHA	~	+
Lateroanterior hypothalamic nucleus	LA	±	±

Peduncular part of lateral hypothalamus	PLH		±
Ventromedial nucleus of the hypothalamus	VMH		+
Arcuate nucleus	Arc	+	++±
Dorsomedial nucleus of the hypothalamus	DMH	±	+±
RFRP-like	RFRP	+	
Medial tuberal nucleus	Mtu	+	++
Posterior hypothalamic nucleus	PH		±
Lateral hypothalamic area	LHA	+	
Medial mammillary nucleus	MM		+
Retromammillary nucleus	RM		+±
Diencephalon (Thalamus)			
Paratenial nucleus of the thalamus	PT	+++	
Reuniens thalamic nucleus	Re		+
Central medial thalamic nucleus	CM	±	+±
Paracentral thalamic nucleus	PC	±	+±
Reticular nucleus	Rt		
Mediodorsal thalamic nucleus	MD	~	
Xiphoid & paraxyphoid thalamic nucleus	Xi/PaXi	++	±
Interanteromedial thalamic nucleus	IAM	~	
Medial habenula	MHb		+++
Lateral habenula	LHb		++
Ventromedial thalamic nucleus	VM		+
Centrolateral thalamic nucleus	CL	+	+±
Intermediodorsal thalamic nucleus	IMD	±	+
Ventral posteromedial nucleus	VPM	±	
Dorsal lateral geniculate nucleus	DLG	+	+
Pregeniculate nucleus	PG		+
Paraventricular nucleus of the thalamus	PVT	+++	+
Parafascicular thalamic nucleus	PF		++±
Intramedullary thalamic nucleus	IMA	±	
Supragenículate thalamic nucleus	SG	++	
Medial geniculate nucleus medial part	MGM	++	
Medial geniculate nucleus dorsal part	MGD	±	+
Mesencephalon			
Zona incerta	ZI		+
Substantia nigra pars compacta	SNC		+
Ventral tegmental area	VTA		+±
Peripeduncular nucleus	PP		±
Intermediate gray superior colliculus	ING		+++
Red nucleus parvicellular part	RPC		~
Superficial gray superior colliculus	SUG		+++
Deep gray superior colliculus	DPG		++
Medial accessory oculomotor nucleus	MA3	±	
Red nucleus magnocellular part	RMC		~
Dorsomedial periaqueductal gray	DMPAG	±	
Lateral periaqueductal gray	LPAG	±	~
Interpeduncular nucleus, intermediate subnucleus	IPI	+±	~
Subbrachial nucleus	SubB	++	±
Nucleus brachium of the inferior colliculus	BIC		+

Dorsal raphe	DR	~	+±
Median raphe	MnR		+±
Interpeduncular nucleus	IP		++±
Ventrolateral periaqueductal gray	VLPAG	+	~
External cortex of the inferior colliculus	ECIC		++±
Dorsal nucleus of the lateral lemniscus	DLL		~
Central gray	CG		+
Met- and Myelencephalon			
Pontine nuclei	Pn	±	+±
Reticulotegmental nucleus of the pons	RtTg		+
Principal sensory trigeminal nucleus	Pr5		+
Parabrachial nucleus	PBN		+
Locus Coeruleus	LC	±	~
Superior vestibular nucleus	SuVe	±	
Medial vestibular nucleus	Mve	+	±
Dorsal cochlear nucleus	DC	~	++
Raphe magnus nucleus	RMg		+±
Spinal trigeminal nucleus	Sp5		+
Prepositus nucleus	Pr	+	±
Accessory nuclei of the abducens and facial nerve	Acs6/7	+	
Area postrema	AP	±	
Cerebellum			
Lobules 9 and 10 of the cerebellar vermis	9/10Cb		±

~ scattered isolated lightly labelled cells
± scattered lightly labelled cells
+ scattered cells not delineating the structure
++ labelled cells delineating the structure
+++ high density of labelled cells
++++ very high density of labelled cells completely filling the structure

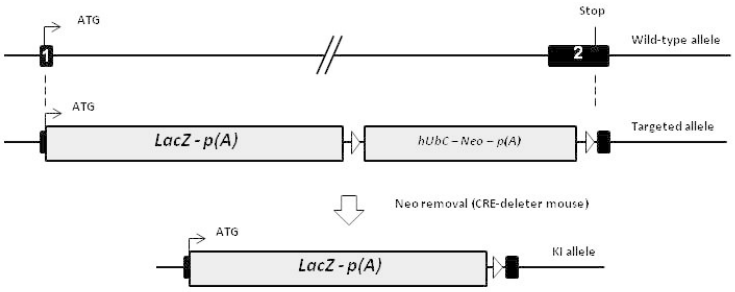

Figure 1. Targeting strategy for the generation of Mtnr1a and Mtnr1b LacZ knock in mice: the wild-type allele is representative of Mtnr1a gene but exon/intron structure and strategy are similar for Mtnr1b. A reporter-selection cassette containing a a) LacZ open reading frame, poly-A site and b) a floxed human Ubiquitin promoter, Neomycine resistance gene, poly-A site sequence, was inserted between the ATG and the stop codon region of the target gene by using a BAC strategy. Mice carrying this targeted allele were generated by ES cell-based/germline transmission. The final knock in mice were derived from the preceding ones by breeding with CRE-deleter mice to remove the selection gene and final segregation of the Cre gene.

254x190mm (96 x 96 DPI)

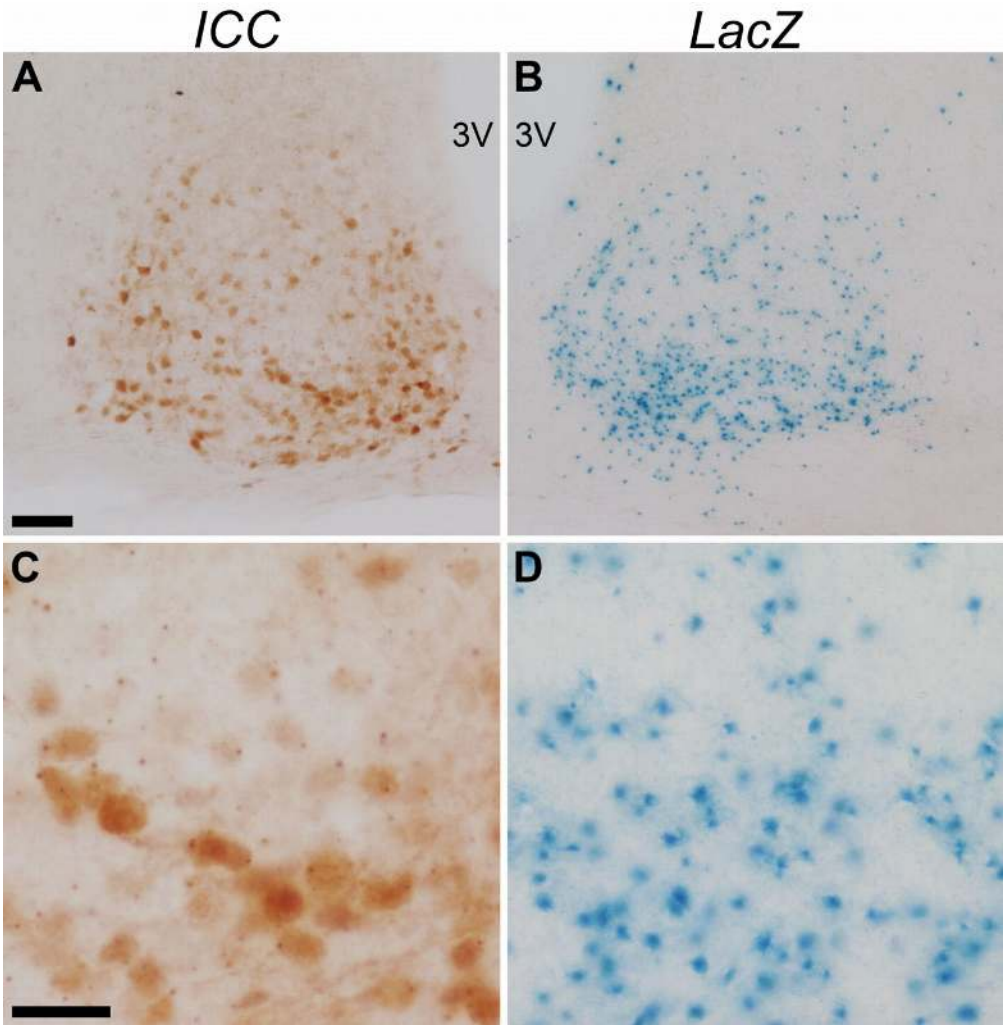

Figure 2. MT1-LacZ expression in the suprachiasmatic nucleus detected by LacZ enzyme histochemistry (A, C) or by LacZ immunohistochemistry (B,D). The LacZ enzyme activity is visualized as strongly stained dots, which most probably are lysosomal accumulations of the transgenic LacZ enzyme (A,C). Immunohistochemical detection of the LacZ protein visualizes LacZ in these same dot-like structures, as well as in the nucleus and cytoplasm of most SCN neurons (B,D). The dot-like structures are bigger in enzyme histochemistry than in immunohistochemistry probably because of the higher diffusion of the X-Gal reaction product compared to the peroxidase diaminobenzidine precipitate.
MT1-LacZ expressing neurons are unevenly distributed in the SCN, with the highest density of MT1-LacZ expressing cells located in the medio-ventral quadrant of the SCN.
Bar in A = 100 μm for A/C, Bar = 50 μm for B/D

109x112mm (300 x 300 DPI)

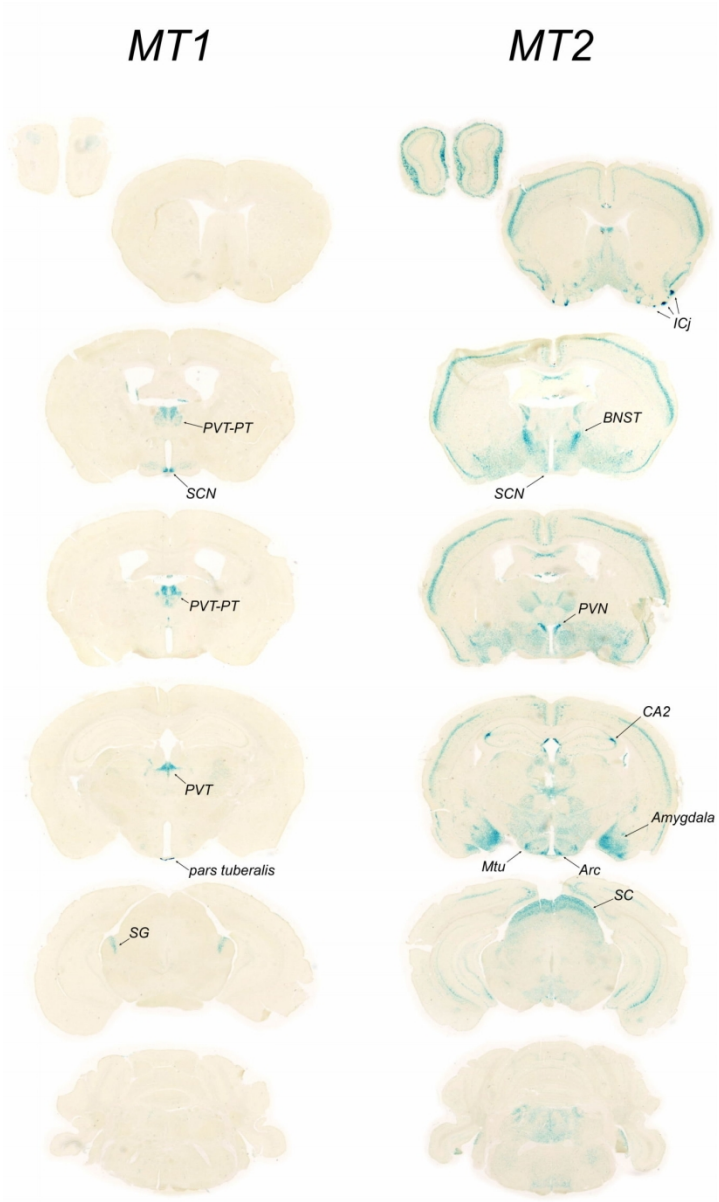

Figure 3. Mapping of MT1-LacZ and MT2-LacZ expression in the mouse brain. Comparable levels are shown for both MT1-LacZ and MT2-LacZ. While MT1-LacZ expression is reduced to only a few discrete structures (most notably the SCN, the PVT-PT complex, the SG and the pars tuberalis), MT2-LacZ expression is much more widespread, particularly in the forebrain.

113x191mm (300 x 300 DPI)

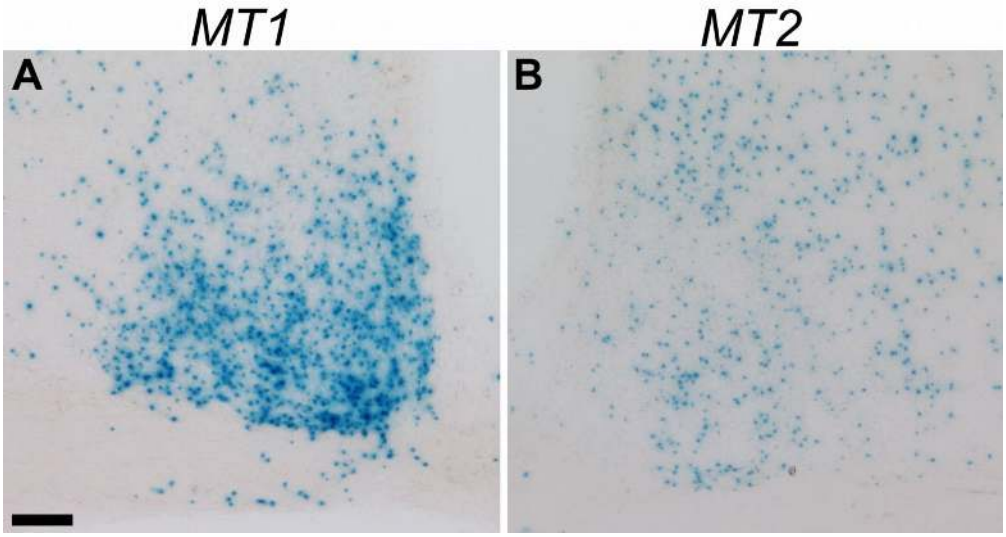

Figure 4. MT1-LacZ (A) and MT2-LacZ (B) expression in the SCN. MT1-LacZ expression in the SCN is higher than MT2-LacZ expression and delineates the boundaries of the SCN. Furthermore, MT2-LacZ expression also is more diffuse in the anterior hypothalamic area.
Bar = 50 μm

113x60mm (300 x 300 DPI)

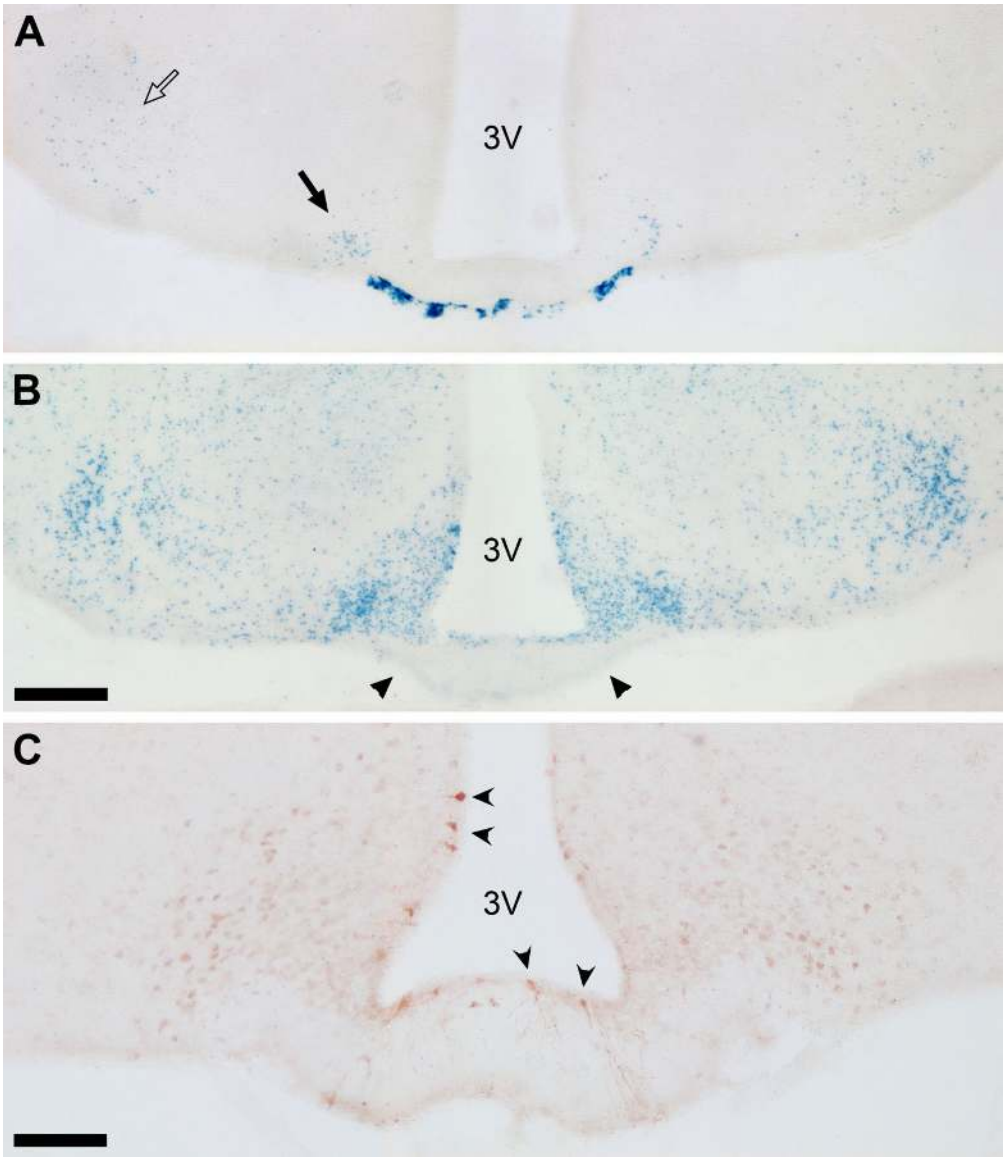

Figure 5. MT1-LacZ (A) and MT2-LacZ (B,C) expression in the mediobasal hypothalamus.
The pars tuberalis of the adenohypophysis displays very high levels of MT1-LacZ expression. Furthermore, MT1-LacZ can be detected in some cells of the arcuate nucleus ((black arrow) and the medial tuberal nucleus (open arrow) particularly in the most rostral regions of these structures (A). MT2-LacZ expression in the mediobasal hypothalamus is much more widespread than MT1-LacZ expression (B), with the notable exception of the pars tuberalis, which is completely devoid of MT2-LacZ staining (double arrow heads). As with all structures where both MT1-LacZ and MT2-LacZ expression can be detected, MT1-LacZ expression is present in a more reduced and discrete subset of cells than MT2-LacZ, as seen here for both the arcuate nucleus and the medial tuberal nucleus. MT2-LacZ expression is also detected in some cells of the ependymal wall, which are identified as tanycytes (arrowheads in C) in LacZ immunohistochemical staining by the processes (C).
Bar in B = 200 μm for A/B
Bar in C = 100 μm

113x131mm (300 x 300 DPI)

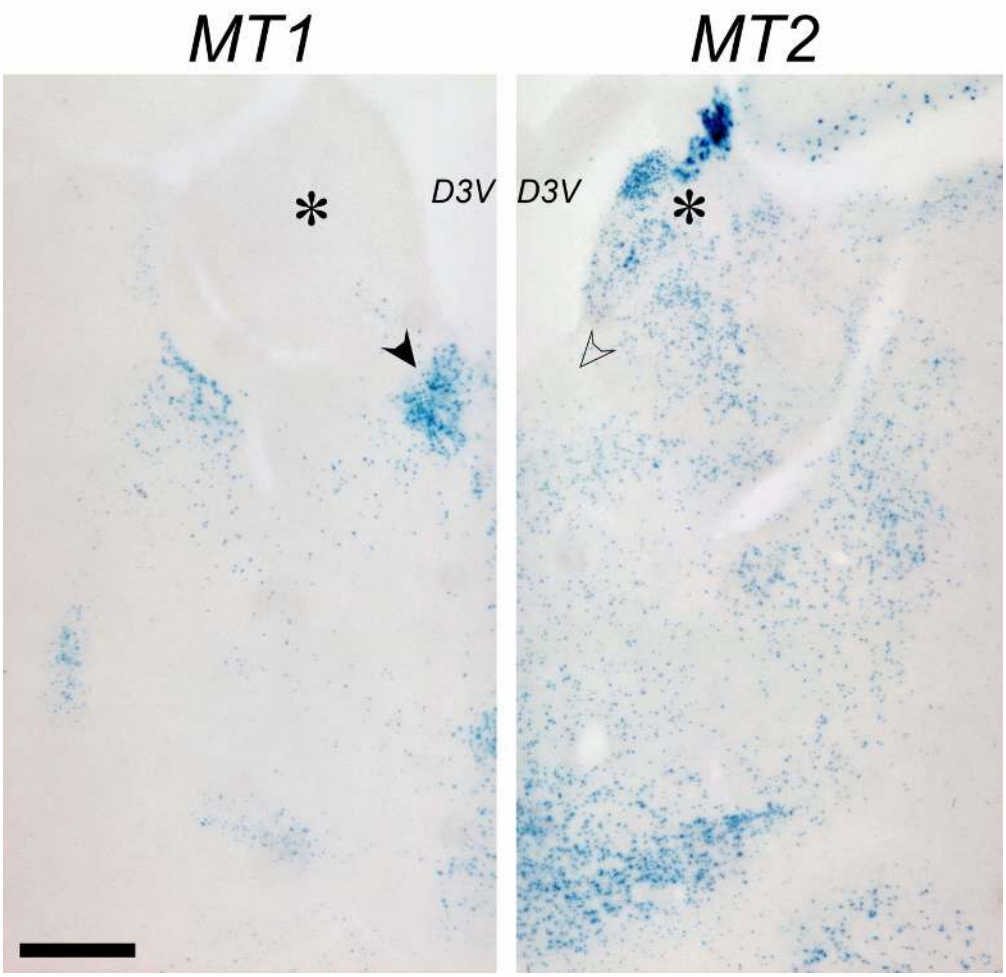

Figure 6. MT1-LacZ and MT2-LacZ expression in the thalamus.
Both MT1-LacZ and MT2-LacZ expression can be seen in various nuclei of the central and dorsal thalamus, as well as the habenula (*). In the paraventricular nucleus of the thalamus, MT1-LacZ expression is particularly high (black arrowhead), while MT2-LacZ expression is reduced to a few cells. (open arrowhead). In almost all other structures, MT1-LacZ expression is reduced to a much smaller subset of cells than MT2-LacZ expression. In the habenula (*), almost no MT1-LacZ expression can be seen.
Bar = 250 μm

113x111mm (300 x 300 DPI)

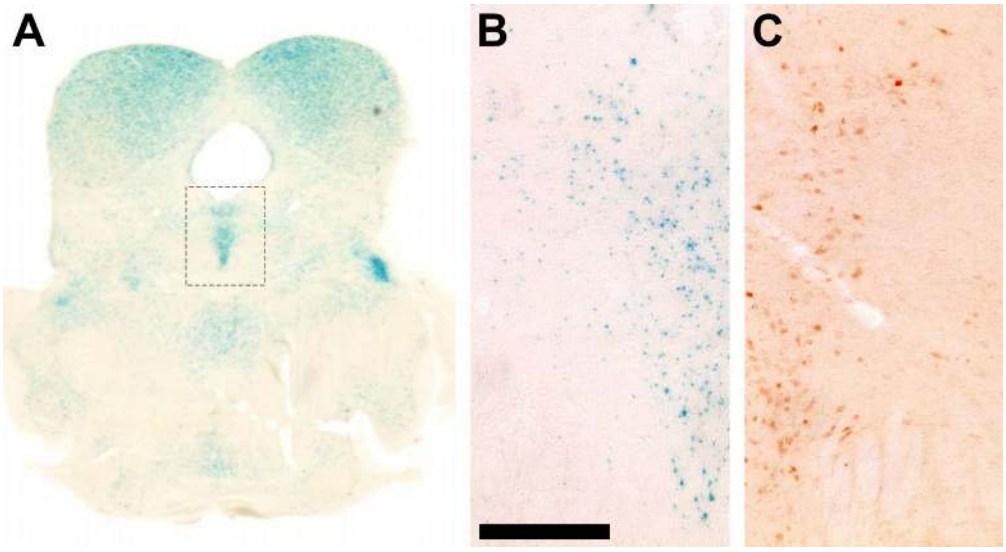

Figure 7. MT2-LacZ expression in the dorsal raphe nucleus by LacZ enzyme histochemistry (A, B) or immunohistochemistry (C). MT2-LacZ expression can be seen in cells delineating an inverted triangular area in the most central part of the dorsal raphe, similar to that observed for serotonergic neurons. Bar = 100 μm

113x61mm (300 x 300 DPI)

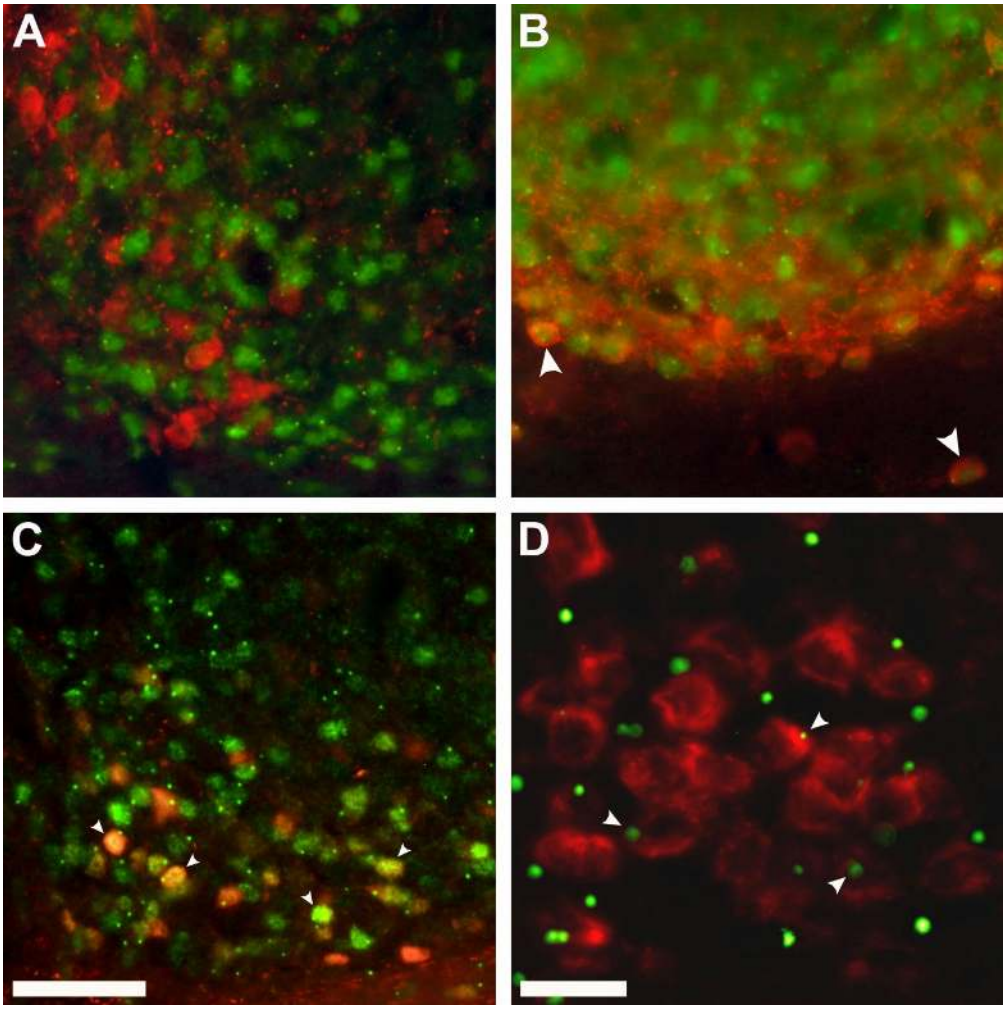

Figure 8. Colocalization of MT1-LacZ immunohistochemistry with neuropeptide markers in the suprachiasmatic nucleus.
(A) Double immunostaining for vasopressin-neurophysin2 (red) and MT1-LacZ (green) show no colocalisation.
(B) Colocalization of vasoactive intestinal peptide (red) and MT1-LacZ (green) in some cells in the most ventral part of the SCN (arrowheads).
(C) In the central part of the SCN, MT1-LacZ (green) can also be seen in some neurons expressing the mRNA for gastrin releasing peptide (red, non-radioactive in situ hybridization). After in situ hybridization, the LacZ immunostaining can only be seen in the dot like structures (arrowheads).
(D) In the central part of the SCN, calretinin (red) can be seen in a number of MT1-LacZ (green) expressing cells (arrowheads). However, there are also cells expressing only either calretinin (red) or MT1-LacZ (green).
Bar in D = 50 μm for A, B and D
Bar in C = 20 μm

113x113mm (300 x 300 DPI)

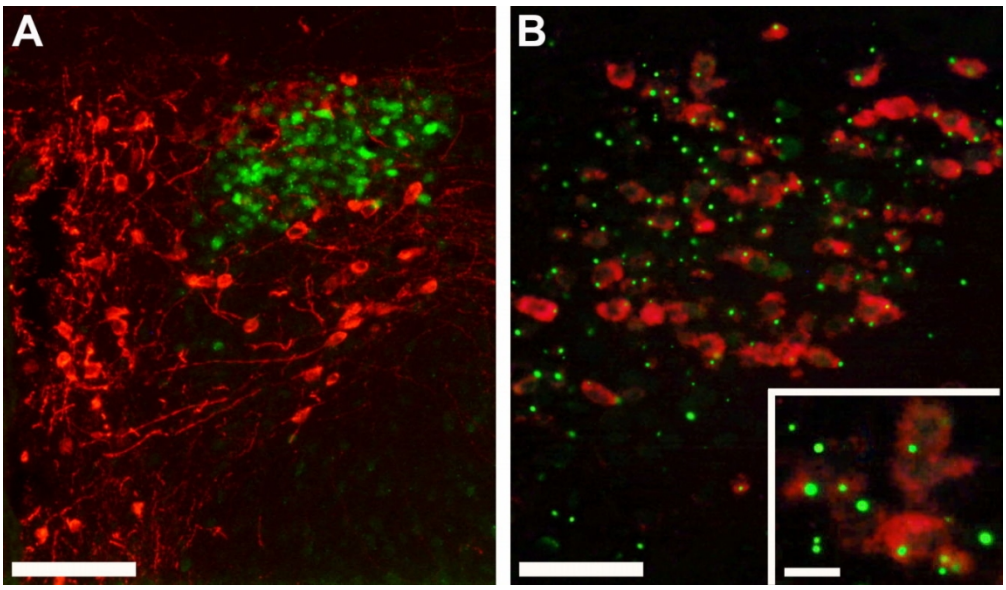

Figure 9. Colocalization of MT2-LacZ immunohistochemistry with neuropeptide markers in the paraventricular nucleus of the hypothalamus.
(A) Double immunostaining for vasopressin-neurophysin2 (red) and MT2-LacZ (green) show no colocalisation. MT2-LacZ expression is present in cells located in the dorsal part of the medial parvicellular subdivision of the paraventricular nucleus.
(B) Double staining for MT2-LacZ (green) and the mRNA of corticotropin releasing hormone (CRH, red) shows that the MT2-LacZ neurons are mostly CRH neurons, although some MT2-LacZ cells are clearly outside of the CRH neurons zone and some CRH neurons do not contain the green dot staining of MT2-LacZ.
Bar in A = 100 µm
Bar in B = 50 µm (insert bar = 20 µm)

113x65mm (300 x 300 DPI)

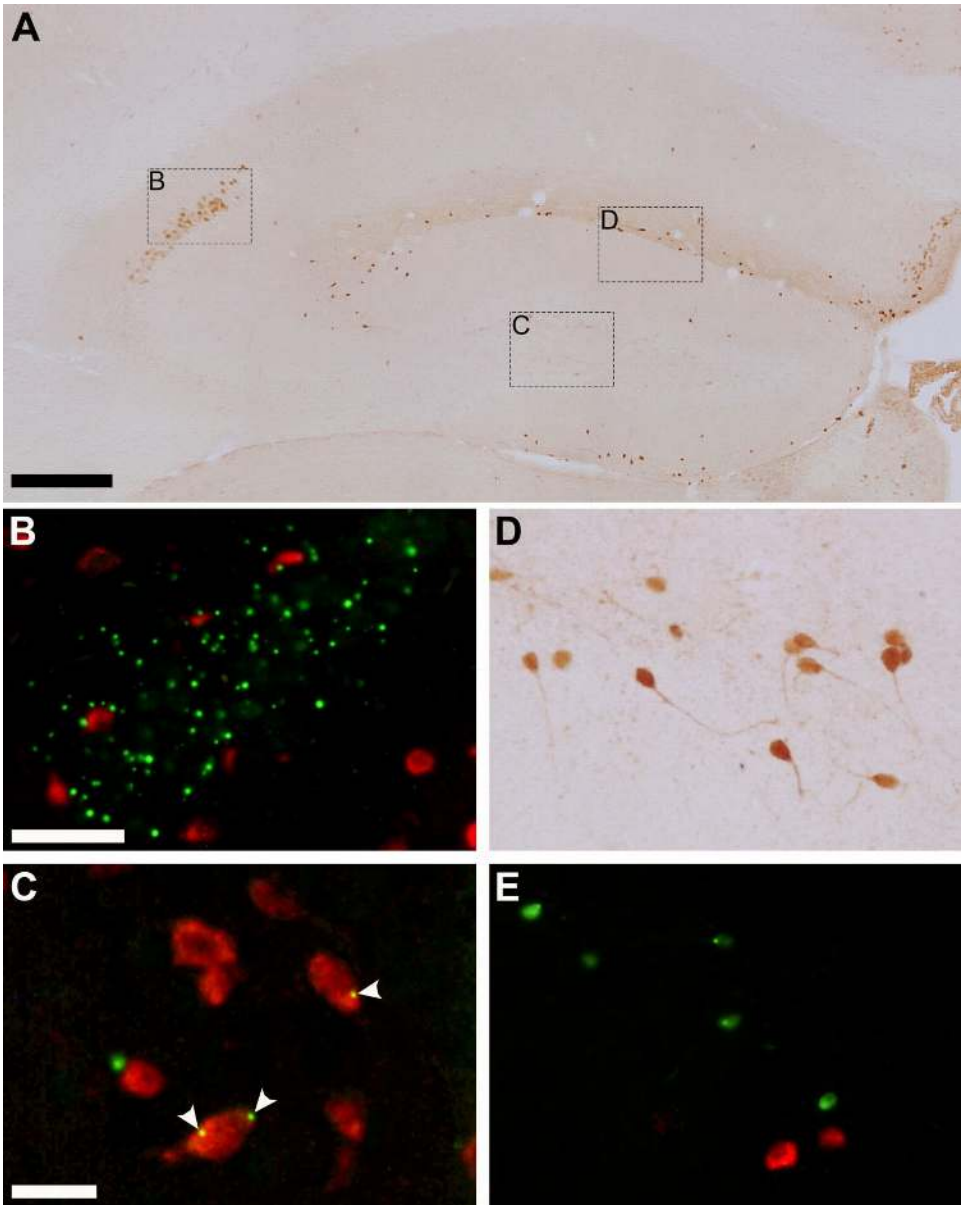

Figure 10. MT2-LacZ expression in the hippocampus.
(A) Particularly dense MT2-LacZ dot-like immunostaining is seen in the CA2 region of the hippocampus (rectangle B). In the hilus of the dentate gyrus, (rectangle C) some lightly stained neurons are present. The strongest staining for MT2-LacZ however is detected in small neurons located in the outer molecular layer of the dentate gyrus (rectangle D). The rectangles show the areas selected for figures 9B, C and D.
(B) Only a few MT2-LacZ positive neurons in the CA2 area co localize with GAD1 or GAD2.
(C) In the hilus of the dentate gyrus, GAD1 or GAD2 can be detected in MT2-LacZ positive neurons (arrowheads).
(D) The small neurons located in the outer molecular layer of the dentate gyrus display a particularly strong immunostaining for LacZ, extending into their neurites.
(E) The MT2-LacZ positive neurons in the outer molecular layer mostly did not express either GAD1 or GAD2.
Bar in A = 250 μm

Bar in B = 50 μm for B, D and E
Bar in C = 25 μm

113x142mm (300 x 300 DPI)

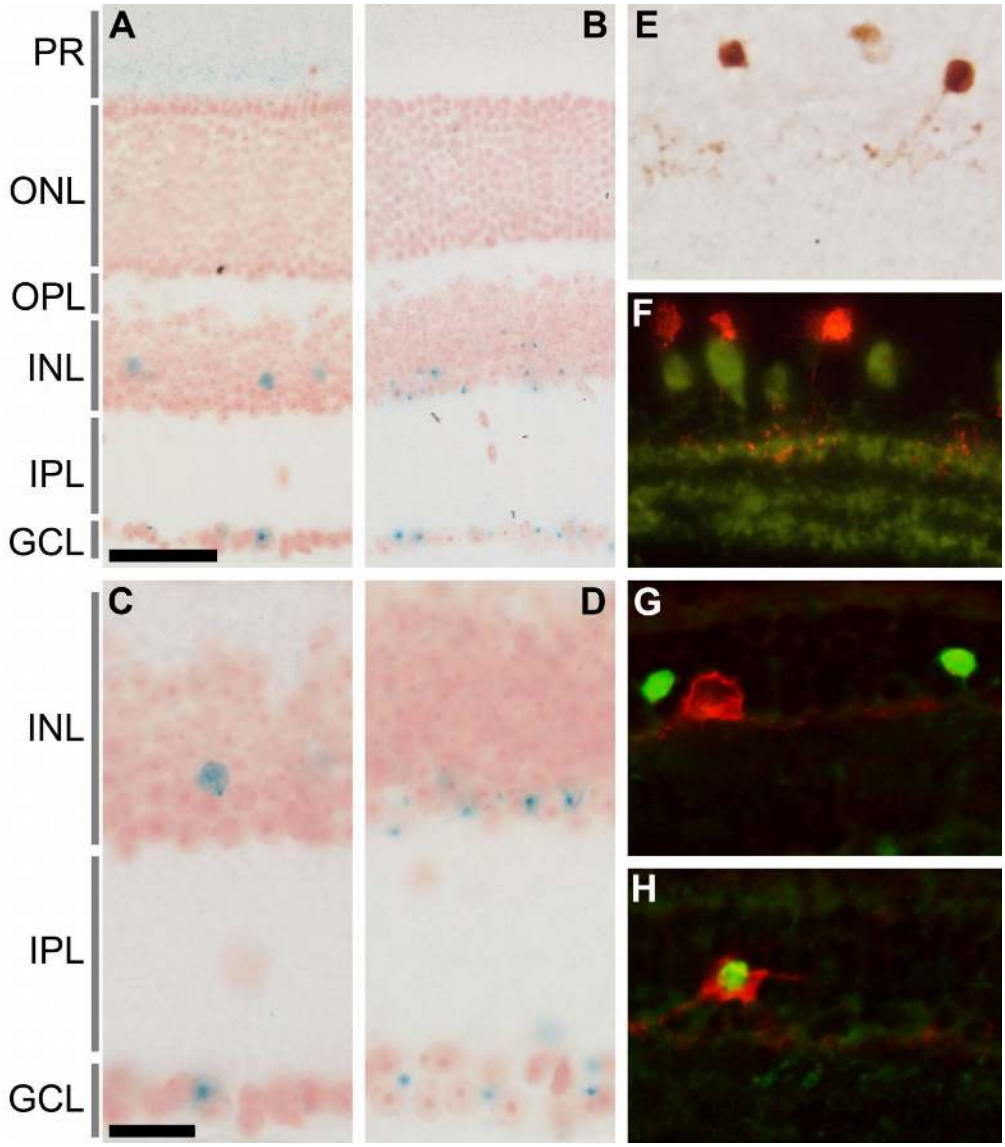

Figure 11. MT1-LacZ and MT2-LacZ expression in the retina. The pink staining of the nuclei is an inverted DAOI stain.
(A) Weak MT1-LacZ enzyme histochemical stain can be seen in the photoreceptor layer (PR). Much stronger enzyme activity is detected in some amacrine cells (fleche SVP) in the inner nuclear layer (INL) and some ganglion cells.(GCL).
(B) MT2-LacZ expression is absent from the photoreceptor layer, but present in some amacrine cells and some ganglion cells.
(C) MT1-LacZ expression in amacrine cells and gangliuon cells. The cell bodies of the amacrine cells expressing MT1-LacZ are located within the inner nuclear layer (INL) away from the boundary of the inner nuclear layer with the inner plexiform layer (IPL).
(D) The cell bodies MT2-LacZ positive amacrine cells are mostly located at the interface between the inner nuclear and plexiform layers.
(E) In the MT1-LacZ amacrine cells, the LacZ immunostaining extends into a neurite ramifying in the upper strata of the inner plexiform layer.
(F) Double immunostaining for MT1-LacZ (red) and calretinin (green) shows that the MT1-LacZ amacrine cells are calretinin negative, and that their neurite ramifies in the upper calretinin layer between strata 1

and 2
(G) Most MT1-LacZ (green) amacrine cells are located higher than the dopaminergic amacrine cells (red, tyrosine hydroxylase).
(H) Only one MT1-LacZ cell (green) colocalized with tyrosine hydroxylase (red) identified
Bar in A = 50 μm for A and C
Bar in B = 20 μm for all other micrographs
PR photoreceptor layer, ONI outer nuclear layer, OPL outer plexiform layer, INL, Inner nuclear layer, IPL, inner plexiform layer, GCL, ganglion cell layer.

113x129mm (300 x 300 DPI)